Hindawi
Journal of Computer Networks and Communications
Volume 2022, Article ID 7143707, 30 pages
https://doi.org/10.1155/2022/7143707

*Research Article*

# Performance Analysis of Underwater Wireless Sensor Network by Deploying FTP, CBR, and VBR as Applications

**K. Sathish,[1] C. V. Ravikumar,[1] Asadi Srinivasulu,[2] and Anand Kumar Gupta[2]**

[1]*SENSE Vellore Institute of Technology, Vellore, India*
[2]*Data Science Research Lab, BlueCrest University, Monrovia, Liberia*

Correspondence should be addressed to Anand Kumar Gupta; head.sp@bluecrest.edu.lr

Received 26 July 2022; Accepted 5 September 2022; Published 23 September 2022

Academic Editor: Giovanni Pau



Oceans cover more than 75% of the planet's land surface, making it the most water-rich place on the Earth. We know very little about oceans because of the extraordinary activities that take place in the depths. Underwater wireless sensors are devices that are able to monitor and record the physical and environmental parameters of their surroundings, as well as transmit these data in a continuous manner to one of the source sensors. The network that is formed by the collection of these underwater wireless sensors is referred to as an underwater wireless sensor network (UWSN). The analysis of performance parameters is thought to be most effectively done with this particular technology. In this paper, we will investigate various performance parameters in a random waypoint mobility model by shifting the maximum speed of a node and altering the number of nodes in the model. These parameters include average transmission delay, average jitter, average pathloss, percentage of utilization, and energy consumed in transmit, receive, and idle modes. The QualNet 7.1 simulator is utilized in order to conduct analyses and performance studies.

## 1. Introduction

The vast majority of our planet is covered by water, but much of this has yet to be discovered [1–4]. This area's exploration has recently seen a significant uptick in activity. Besides being rich in valuable resources, it has also played an important role in defence, transportation such as ships, and natural resources such as oil pipelines.The researcher's most pressing concern in areas such as oceans, seas, and the lakes, contain enormous amounts of naturally occurring data [5, 6]. The developers have been able to gather and analyse a large amount of data to some extent by creating a variety of UWSN protocols for the underwater environment [7–10].The results of prior studies of UWSN, as described in the area background below, serve as a foundation for research in this area. Figure 1 shows that the general structure of underwater wireless communication consists of member nodes, cluster nodes, cluster heads, radio channel, and acoustic channel along with the underwater surface and an onshore link.

Wireless sensor networks (WSNs) are a type of ad-hoc wireless network that is used to offer a wireless communication set-up, i.e., as an application underwater wireless communication [11]. Ad-hoc On-demand Distance Vector (AODV), dynamic source routing protocol (DSR), Dynamic Manet on Demand Routing Protocol (DYMO), Location Aided Routing (LAR1), Bellman Ford, Optimized Link State Routing Protocol (OLSR), Fisheye, Source Tree Adaptive Routing Optimum Routing Approach (STAR-ORA), Zone Routing Protocol (ZRP), Source Tree Adaptive Routing-Least Overhead Routing Approach (STAR-LORA), and others are some of the routing protocols available for ad-hoc networks [12].

The mobility model depicts how nodes move and how their location, velocity, and acceleration change over time. It is critical to simulate and evaluate the protocol performance of a new network protocol when researching it. The mobility model and the communicating traffic pattern are two important parameters in protocol simulation. User movement patterns are described by mobility models. Models of traffic

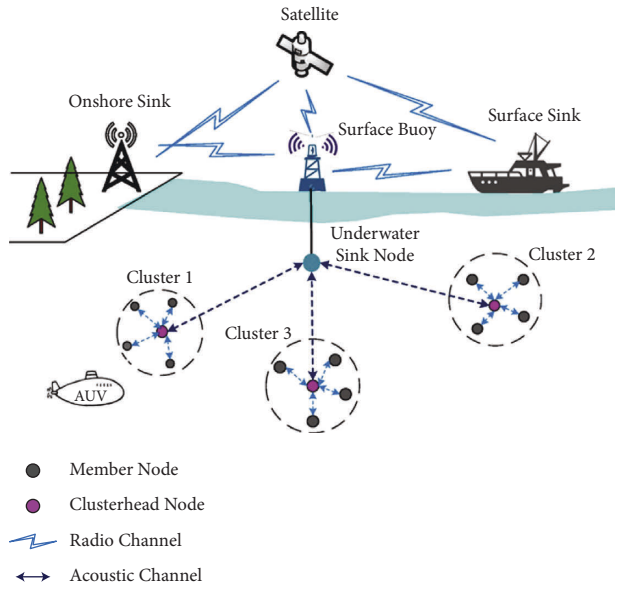


Figure 1: General structure of underwater wireless communication.

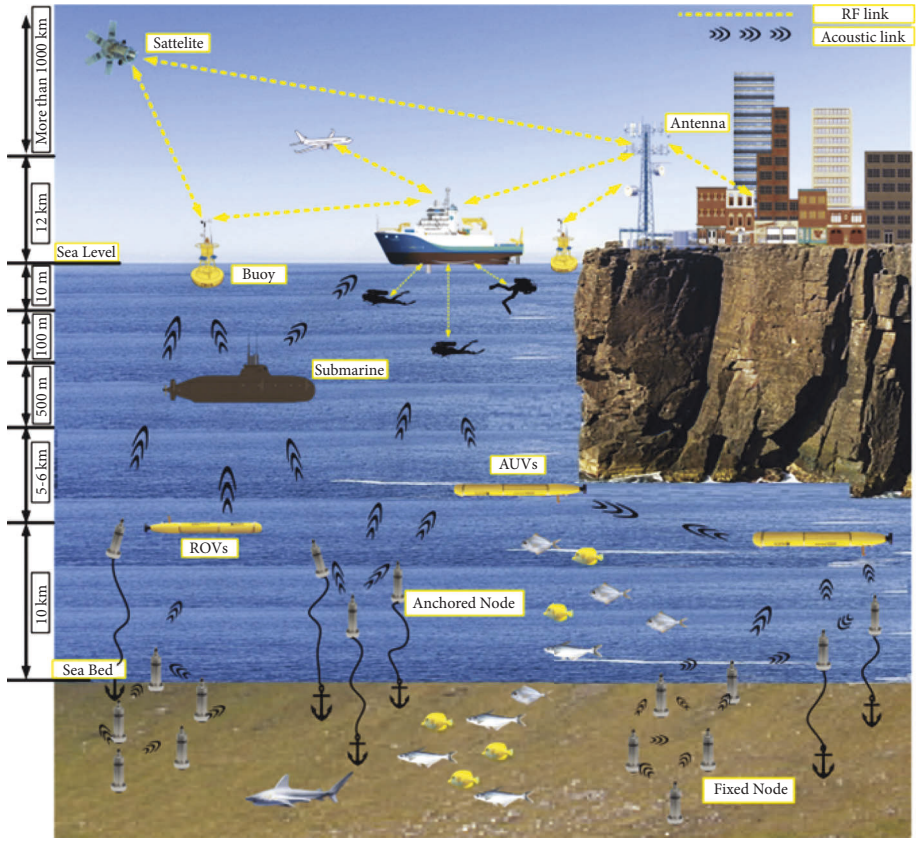


Figure 2: Real scenario of underwater wireless Communication with various nodes.

describe the state of mobile services [13–17]. Figure 2 represents the real scenario of underwater wireless communication with various nodes in different ranges of frequencies under sea level as well as above sea level.

When contemplating the use of underwater sensor networks, one must ensure that the potential difficulties posed by the surrounding subsurface environment are given the attention and consideration they deserve [18–20]. Major challenges posed by the host conditions include continuous node movement and three-dimensional topology. In addition, many of the applications that are used underwater, such as those for detection or rescue missions, have a tendency to be of an ad-hoc nature [20–26].

The main contribution of the manuscript is highlighted as follows:

(i) To implement routing protocol for underwater wireless sensors network (UWSN).

(ii) To compare the STAR-LORA and fisheye routing protocol with standard routing protocols in literature, namely, AODV, DSR, DYMO, LAR1, Bellman Ford, OLSR, Fisheye, STAR-ORA, and ZRP.

(iii) To analyse the energy efficiency of the routing protocol with the increase number of underwater wireless sensors nodes.

(iv) To analyse the trade-off between average transmission delay, average jitter, utilisation rate, and energy in transmit and receive modes.

(v) To recommend appropriate routing protocol based on the targeted performance metric for underwater wireless sensors network.

Sections 2 covers design and simulation parameters. Section 3 gives the methodology of network scenario. In Section 4, we present investigational results. Section 5 provides simulation results. Finally, we have concluded in Section 6.

## 2. Design and Simulation Parameters

Generally, the design of UWSN is considered in various simulation tools such as Network Simulator, OPNET, OMNET, MATLAB, QUALNET, etc., [27–33]. In this proposed network, USWN is designed in QualNet simulator with various design parameters of UWSN as user friendly. The below mentioned parameters are the performance parameters of UWSN network in different applications. UWSNs have many research issues that affect design and performance of overall network such as long propagation delay, high energy consumption, and high dynamic topology [34, 35].

*2.1. Average Transmission Delay.* The information travelled from the source to the destination in successful transmission is referred as an average transmission delay.

*2.2. Percentage of Utilization.* A communication channel's throughput is the percentage of packets that are effectively transferred from the transmitting node to the receiving node.

*2.3. Average Jitter.* It refers to the difference in time that occurs between individual packets as a result of changes in route or network congestion. In order to a routing protocol to work more effectively, it should be lower. Congestion on a network, changes in its routing, or timing drift all can contribute to jitter by causing a delay in transmission between individual packets.

*2.4. Average Path Loss.* The term "path loss," also known as "path attenuation," refers to the gradual reduction in power density that any electromagnetic wave experiences as it travels through space.

*2.5. Energy Consumption.* Energy consumption is the amount of power expended by nodes in the transmission of data from their point of origin to their point of destination.

## 3. Methodology of Network Scenario

*3.1. Existing Network.* There are approachable existing networks that are available with CBR as a deployment application. In this proposed network, FTP and VBR are considered along with CBR and finally compared the parameters with all the three FTP, CBR and VBR applications [13, 22, 26, 36–38].

*3.2. Proposed Network.* The proposed scenario is designed in Qualnet 7.1 Simulator with an area of 1500 by 1500 sq.mts. There are 60 nodes considered in which 15 are node devices, 25 are ship devices, and 20 are sensor devices which are connected with respect to file transfer protocol (FTP), constant bit rate (CBR), and variable bitrate (VBR) applications. The simulation runs for a total of 500 seconds. The node mobility model is set to random waypoint mobility with a minimum speed of 1.5 m/sec and a maximum speed of 3 to 10 m/sec. The initial routing protocol is AODV and followed by DSR, DYMO, LAR1, Bellman Ford, OLSR, Fisheye, STAR-ORA, ZRP, and STAR-LORA. We examine the graphs in simulator after running the test. Thus, we obtain the necessary performance metrics: average transmission delay, average Jitter, average pathloss, percentage of utilization, and energy consumed in transmit, receive and idle modes. Figure 3 and Figure 4 represent proposed scenario of underwater wireless communication with various nodes in both X–Y and 3D- Visualization. Figure 5 and Figure 6 represent proposed scenario of underwater wireless communication with various nodes in both X–Y and 3D-Visualization [39, 40].

Clustering algorithms can make the use of methods that are either centralised or decentralised in order to select the CHs that will be the most helpful. When using centralised approaches, all of the necessary criteria for selecting CHs are compiled at a single node (often the BS) where they are then subjected to comparison, analysis, and processing. The expense of centralised techniques can be prohibitive for large and/or dynamic networks, especially when CHs are reselected on a frequent basis. This is the case despite the fact that their findings have the potential to be universal due to the fact that they compare all nodes. The transmission of several management packets, which can place a significant strain on a network's resources, is required by such systems. The overhead of distributed techniques is reduced, but the selected CHs that these systems produce are often unable to match all of the requirements of the network because of the limited network information that they have (i.e., only neighbour nodes).

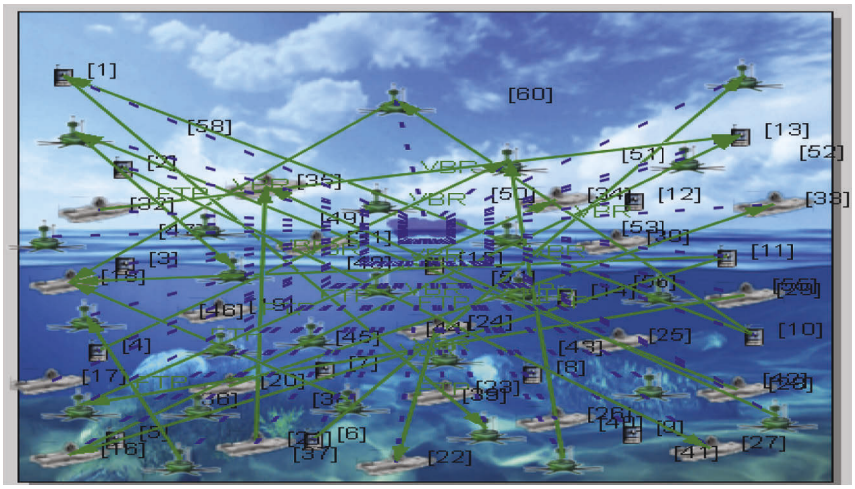


Figure 3: Proposed scenario of underwater wireless communication with various nodes in X-Y visualization.

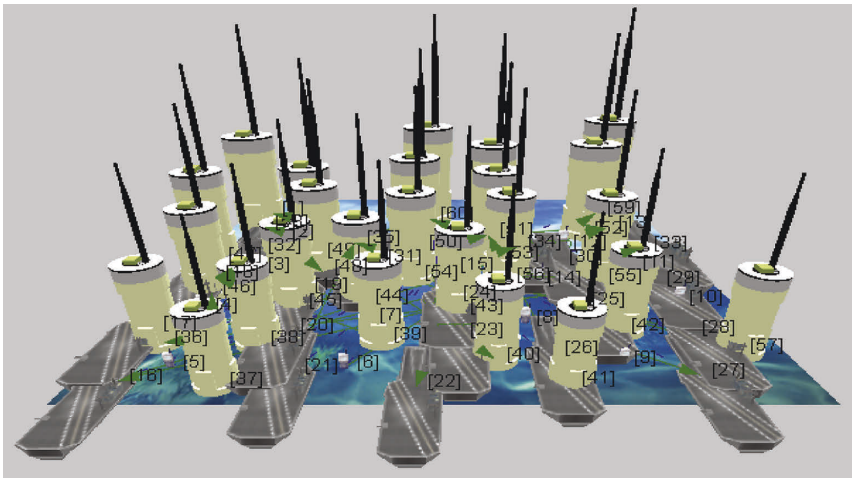

Figure 4: Proposed scenario of underwater wireless communication with various nodes in 3D-visualization.

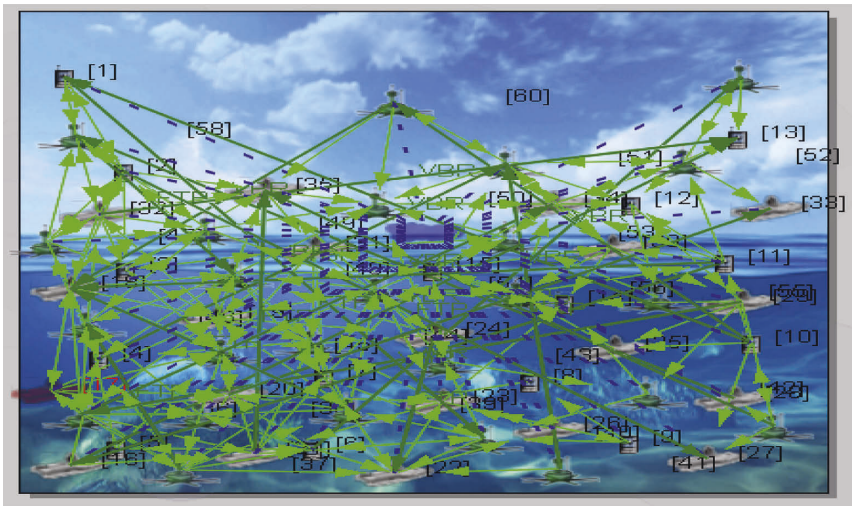


Figure 5: Runtime proposed scenario of underwater wireless communication with various nodes in X-Y visualization.

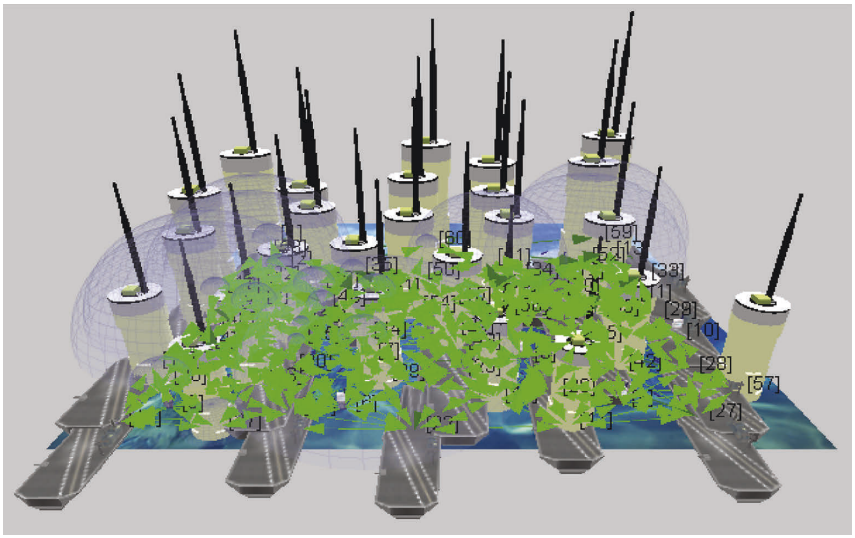

Figure 6: Runtime proposed scenario of underwater wireless communication with various nodes in 3D-visualization.

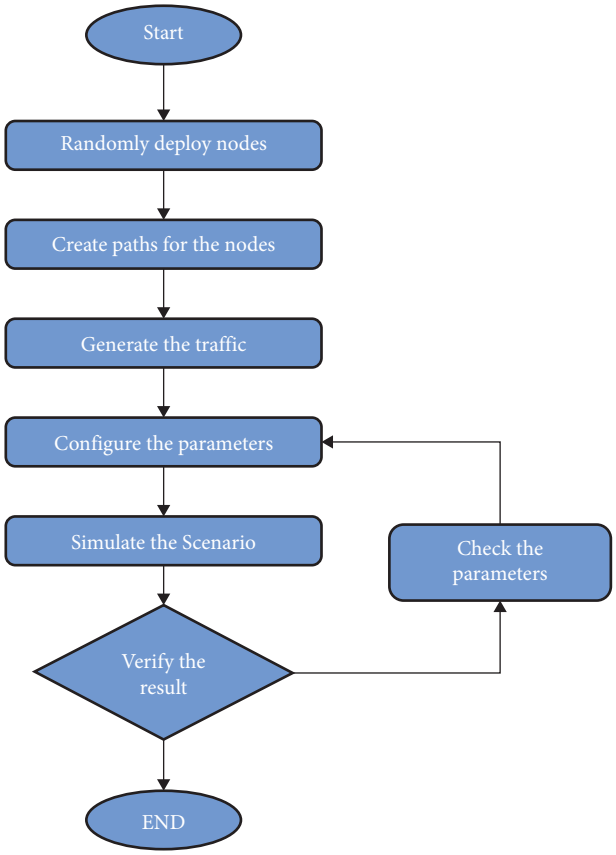


Figure 7: Flow chart of the proposed scenario of UWSN.

*3.3. Random Waypoint Mobility Model.* This model is typically used to assess the effectiveness of routing protocols in UWSN due to its simplicity and wide availability. The remote node in this proposed model utilises any random location as destination and moves in a randomly selected straight line through a constand speed. The amount of time taken by the node to reach at its destination is termed as length and is determined by the pause period of the remote node. This is repeated by the node throughout the simulation process [15].

## 4. Investigational Results

In this section, the flow chart for the proposed UWSN network scenario is shown in Figure 7. In the flow chart, based upon the nodes, deployments are done randomly and the paths are created for nodes. Then after, it needs to generate the traffic for configuring the required parameters and simulate the UWSN testing enviornment.

Also, the investigational results such as average transmission delay, average jitter, avrage path loss, percentage of utilization, engery consumed in transmit, rereive, and idle modes are obtained and discussed in below Figures 8(a)–17(g) represents FTP application. Figures 18(a)–27(g) describes VBR application for various routing protocols such as AODV, DSR, DYMO, LAR1, Bellman Ford, OLSR, Fisheye, STAR-ORA, ZRP and STAR-LORA with FTP, CBR and VBR applicatoins. These results are taken from Qualnet simulator under different application layers.

## 5. Simulation Results

Here are the results of finding performance parameters of proposed UWSN network in FTP, CBR, and VBR applications. See Figure 28.

*5.1. Performance Parameters.* The following are performance parameters of UWSN network in FTP, CBR, and VBR applications.

*5.1.1. Energy (Milli Watt Hour-mWh) Consumed in Transmit Mode by AODV, DSR, DYMO, LAR1, Bellman Ford, OLSR, Fisheye, STAR-ORA, ZRP, and STAR-LORA Routing Protocols.* Comparison of AODV, DSR, DYMO, LAR1, Bellman Ford, OLSR, Fisheye, STAR-ORA, ZRP, and STAR-

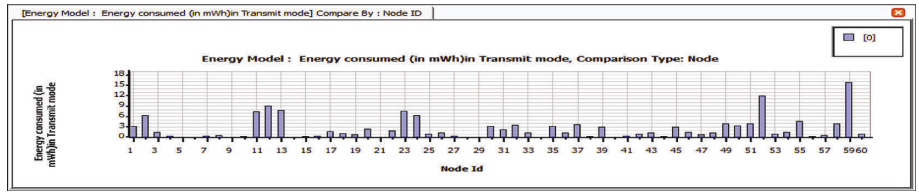


(a)

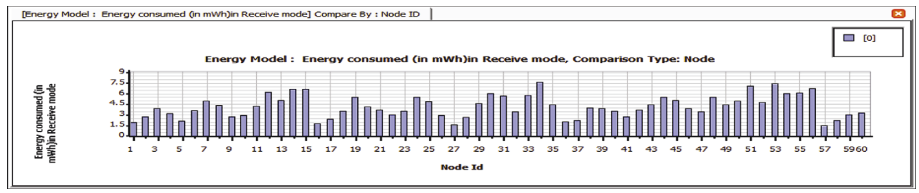


(b)

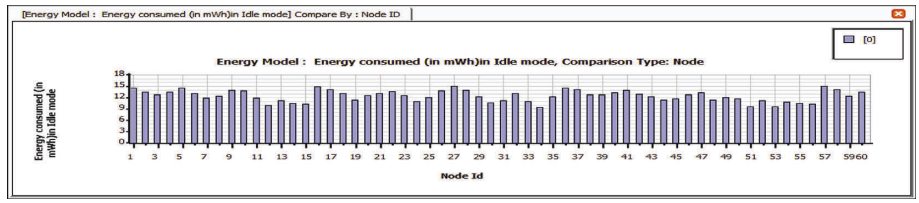


(c)

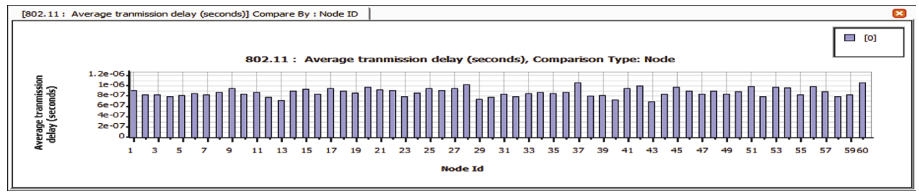


(d)

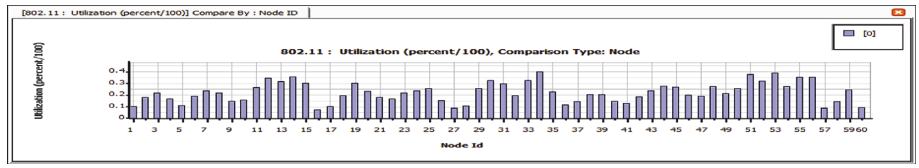


(e)

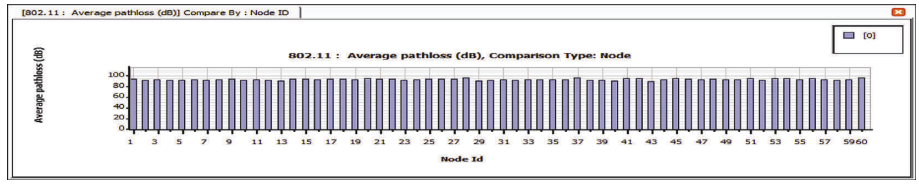


(f)

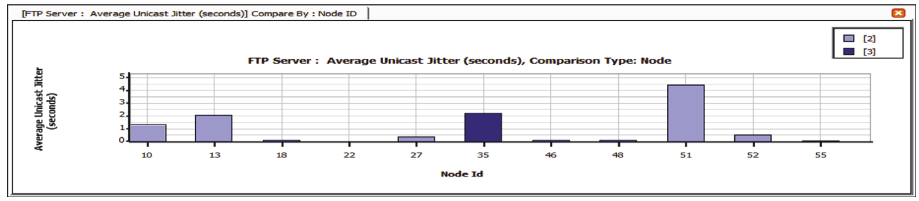


(g)

Figure 8: (a) Transmit mode energy consumption of AODV for FTP deployment. (b) Receive mode energy consumption of AODV for FTP deployment. (c) Idle mode energy consumption of AODV for FTP deployment. (d) Average transmission delay of AODV for FTP deployment. (e) Percentage of utilization of AODV for FTP deployment. (f) Average pathloss of AODV for FTP deployment. (g) Average unicast jitter of AODV for FTP deployment.

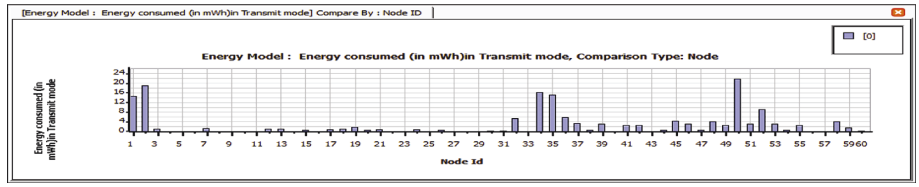


(a)

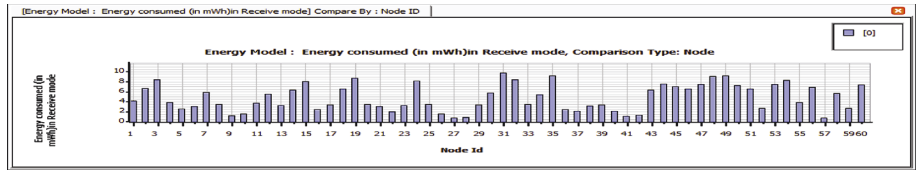


(b)

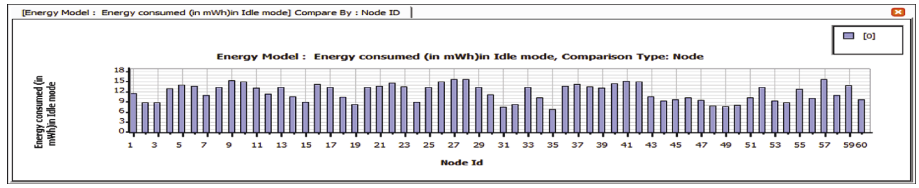


(c)

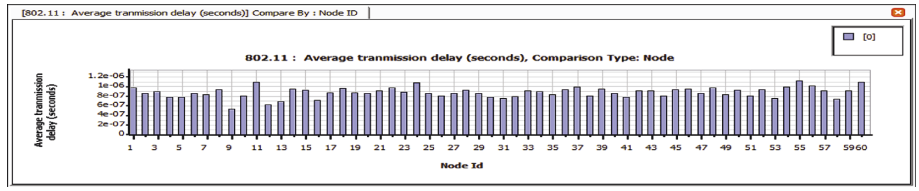


(d)

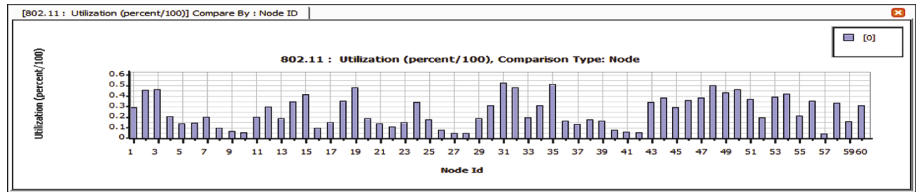


(e)

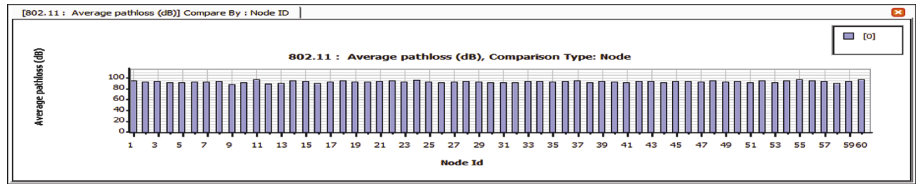


(f)

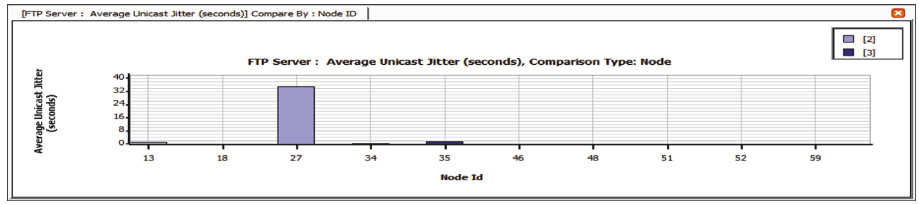


(g)

Figure 9: (a) Transmit mode energy consumption of DSR for FTP deployment. (b) Receive mode energy consumption of DSR for FTP deployment. (c) Idle mode energy consumption of DSR for FTP deployment. (d) Average transmission delay of DSR for FTP deployment. (e) Percentage of utilization of DSR for FTP deployment. (f) Average pathloss of DSR for FTP deployment. (g) Average unicast jitter of DSR for FTP deployment.

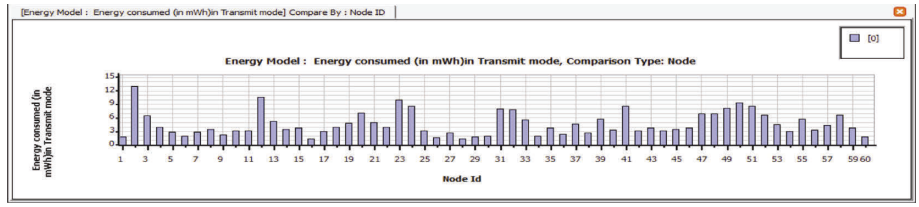


(a)

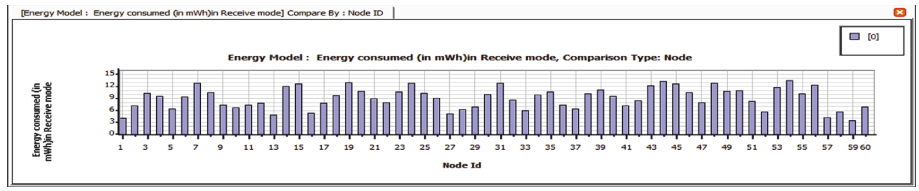


(b)

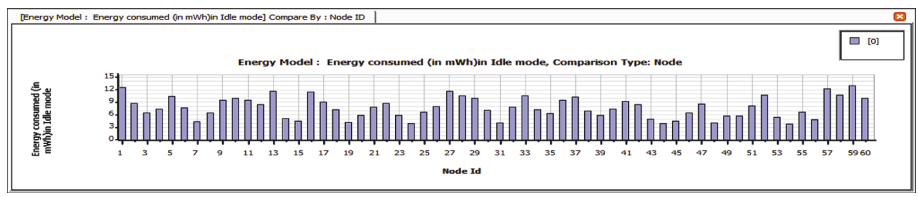


(c)

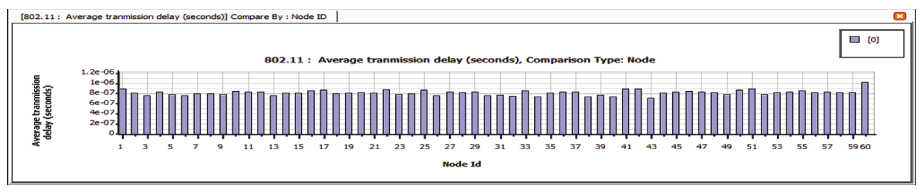


(d)

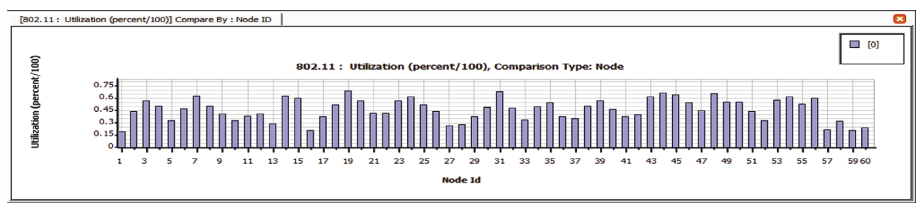


(e)

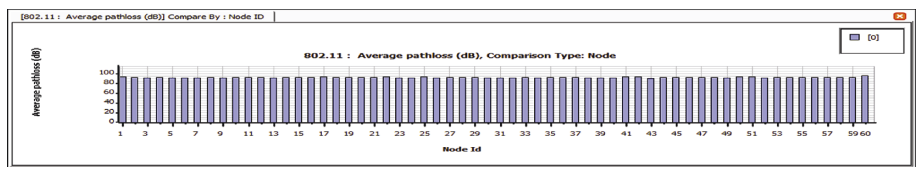


(f)

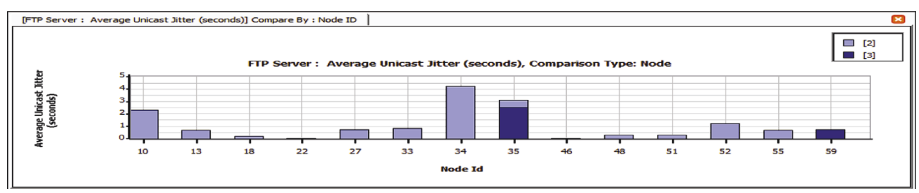


(g)

Figure 10: (a) Transmit mode energy consumption of DYMO for FTP deployment. (b) Receive mode energy consumption of DYMO for FTP deployment. (c) Idle mode energy consumption of DYMO for FTP deployment. (d) Average transmission delay of DYMO for FTP deployment. (e) Percentage of utilization of DYMO for FTP deployment. (f) Average pathloss of DYMO for FTP deployment. (g) Average unicast jitter of DYMO for FTP deployment.

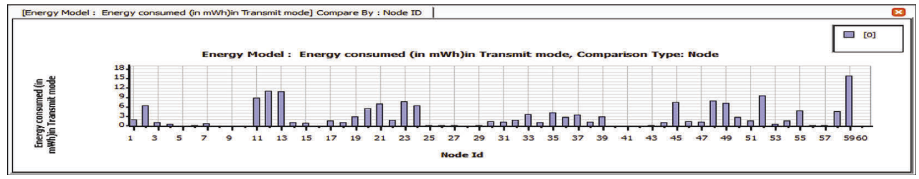


(a)

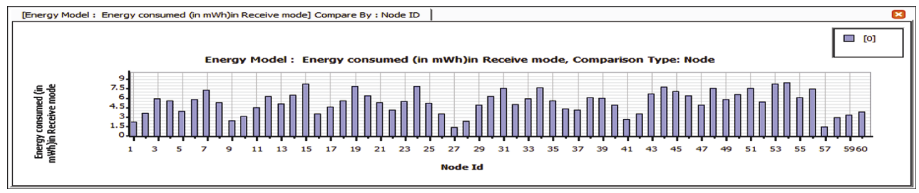


(b)

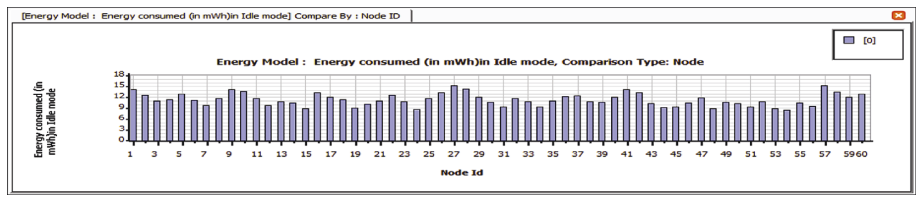


(c)

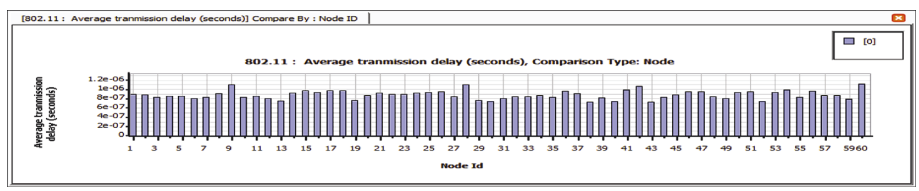


(d)

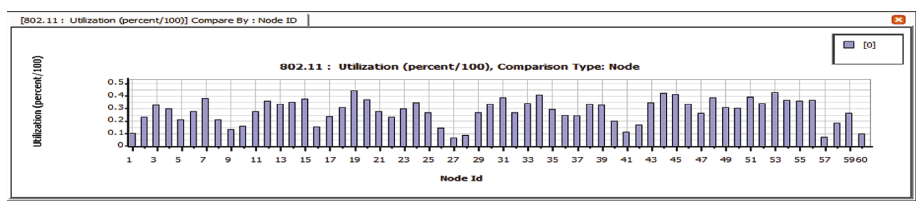


(e)

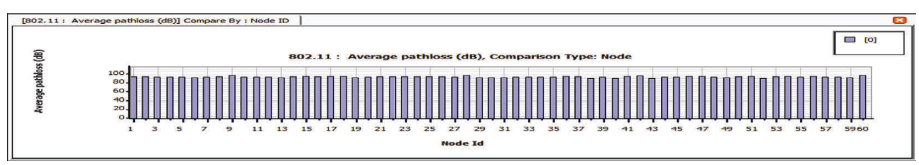


(f)

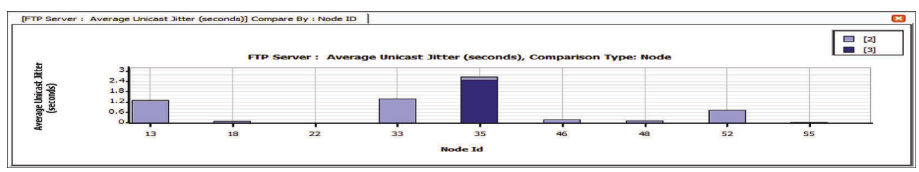


(g)

FIGURE 11: (a) Transmit mode energy consumption of LAR1 for FTP deployment. (b) Receive mode energy consumption of LAR1 for FTP deployment. (c) Idle mode energy consumption of LAR1 for FTP deployment. (d) Average transmission delay of LAR1 for FTP deployment. (e) Percentage of utilization of LAR1 for FTP deployment. (f) Average pathloss of LAR1 for FTP deployment. (g) Average iitter of LAR1 for FTP deployment.

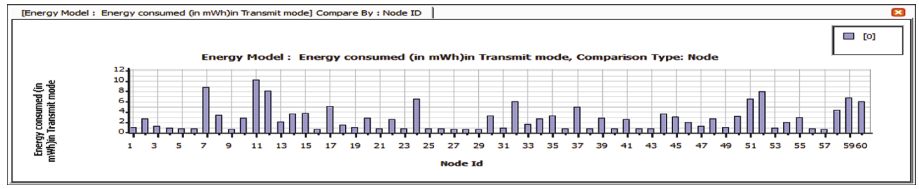


(a)

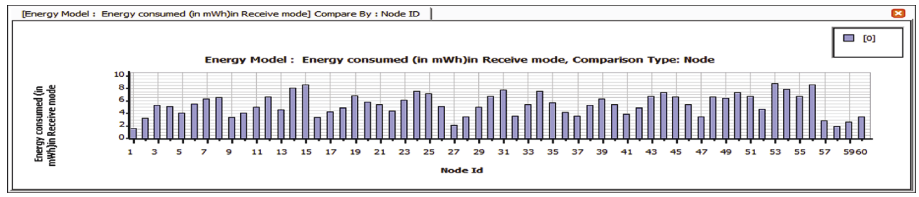


(b)

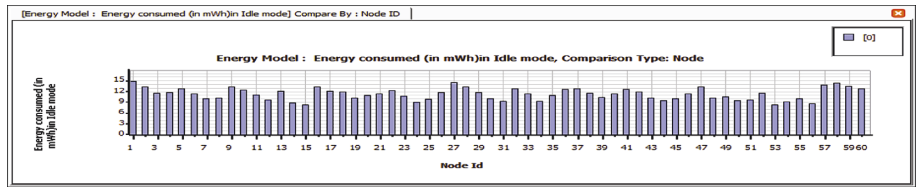


(c)

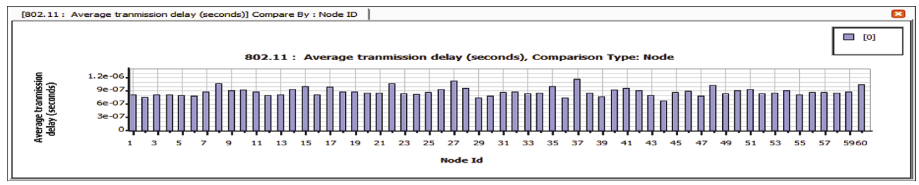


(d)

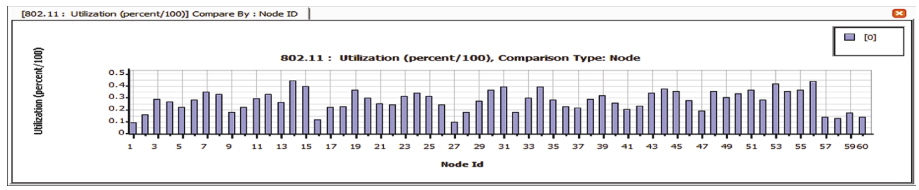


(e)

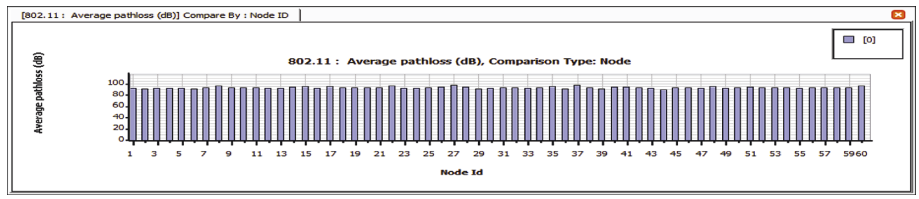


(f)

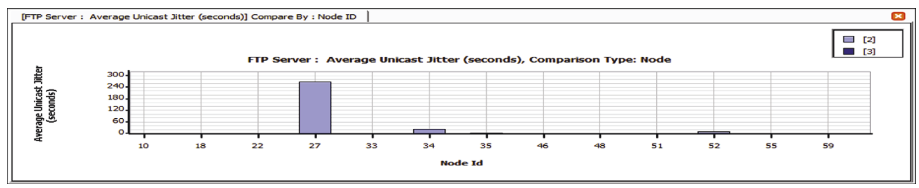


(g)

FIGURE 12: (a) Transmit mode energy consumption of OLSR for FTP deployment. (b) Receive mode energy consumption of OLSR for FTP deployment. (c) Idle mode energy consumption of OLSR for FTP deployment. (d) Average transmission delay of OLSR for FTP deployment. (e) Percentage of utilization of OLSR for FTP deployment. (f) Average pathloss of OLSR for FTP deployment. (g) Average jitter of OLSR for FTP deployment.

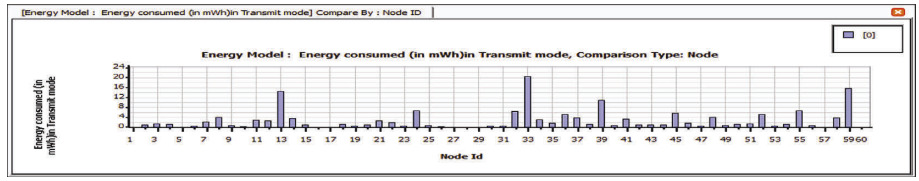


(a)

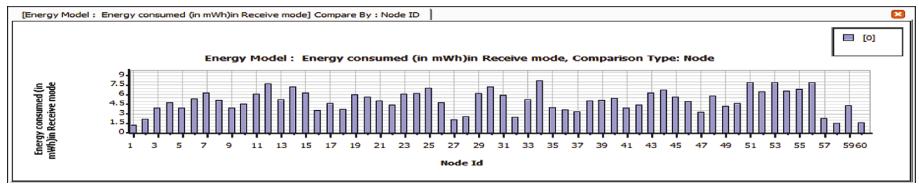


(b)

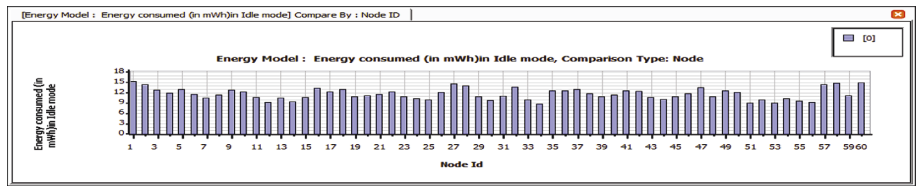


(c)

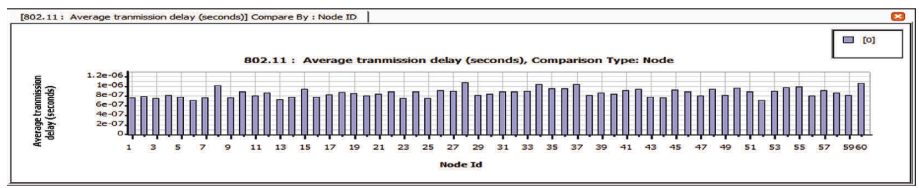


(d)

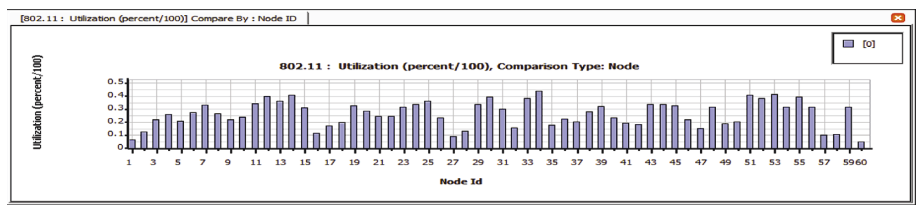


(e)

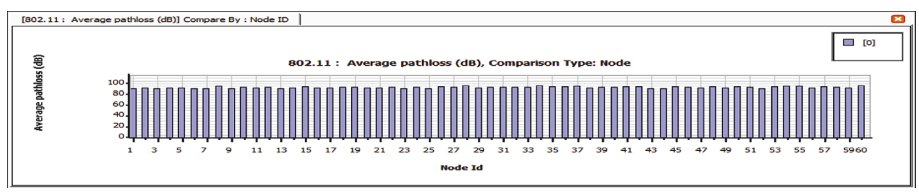


(f)

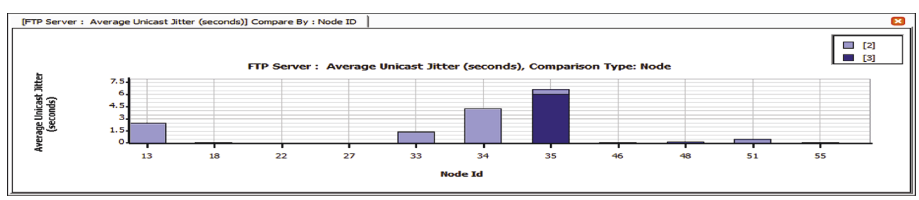


(g)

Figure 13: (a) Transmit mode energy consumption of BELLMAN FORD for FTP deployment. (b) Receive mode energy consumption of BELLMAN FORD for FTP deployment. (c) Idle mode energy consumption of BELLMAN FORD for FTP deployment. (d) Average transmission delay of BELLMAN FORD for FTP deployment. (e) Percentage of utilization of BELLMAN FORD for FTP deployment. (f) Average pathloss of BELLMAN FORD for FTP deployment. (g) Average jitter of BELLMAN FORD for FTP deployment.

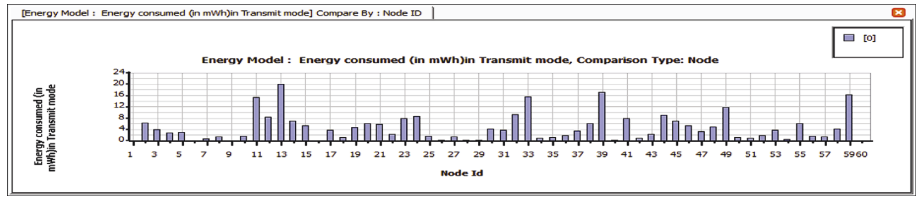


(a)

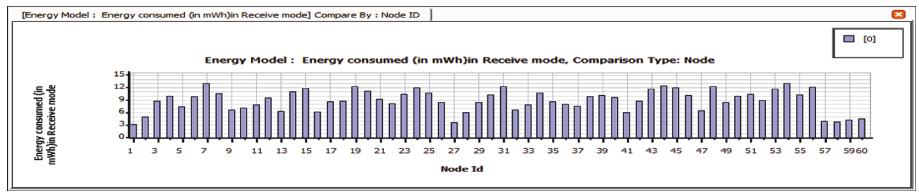


(b)

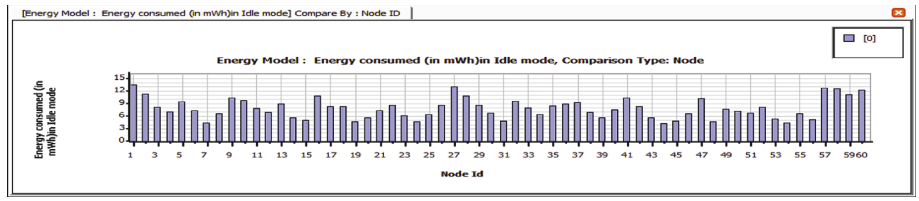


(c)

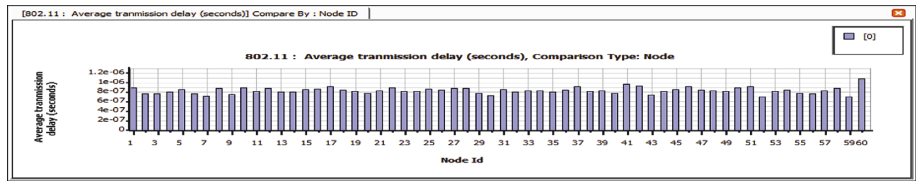


(d)

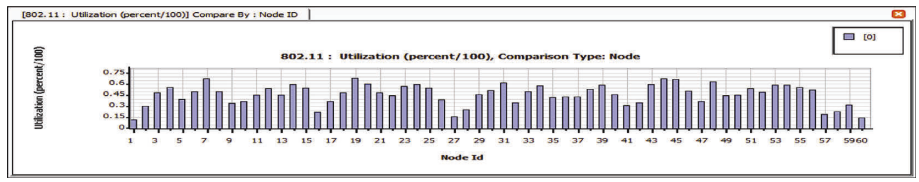


(e)

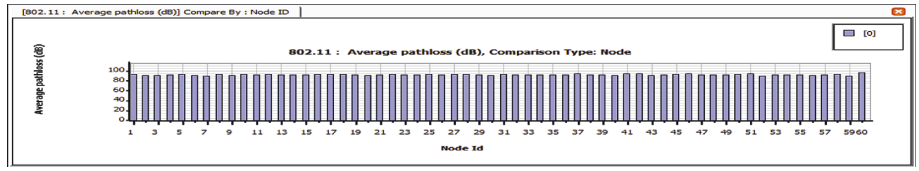


(f)

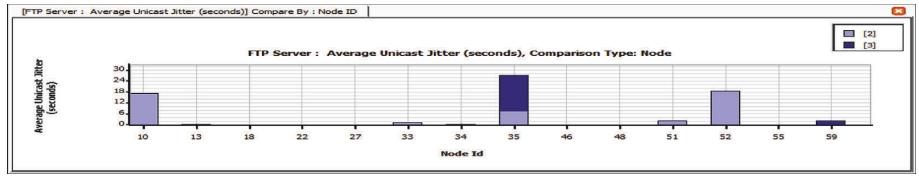


(g)

Figure 14: (a) Transmit mode energy consumption of Fisheye for FTP deployment. (b) Receive mode energy consumption of Fisheye for FTP deployment. (c) Idle mode energy consumption of Fisheye for FTP deployment. (d) Average transmission delay of Fisheye for FTP deployment. (e) Percentage of utilization of Fisheye for FTP deployment. (f) Average pathloss of Fisheye for FTP deployment. (g) Average jitter of Fisheye for FTP deployment.

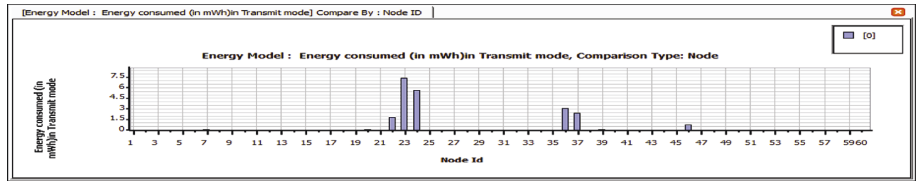


(a)

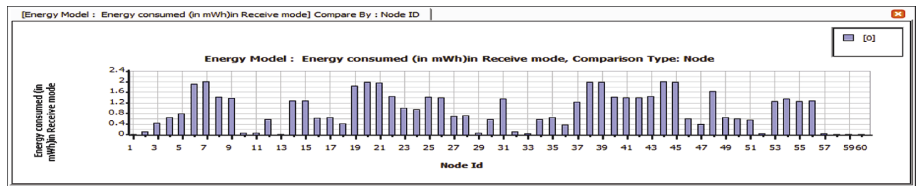


(b)

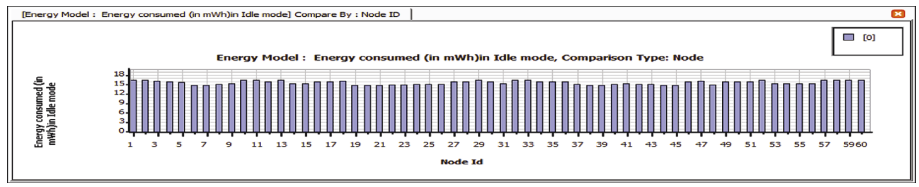


(c)

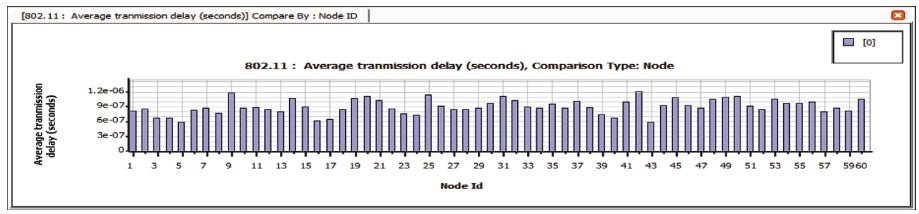


(d)

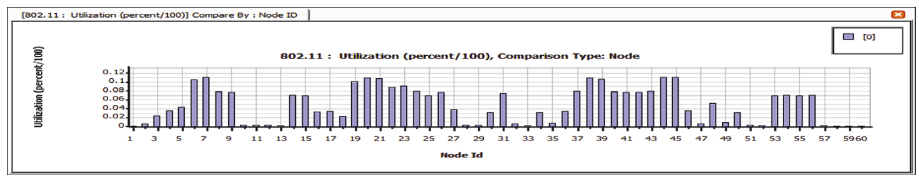


(e)

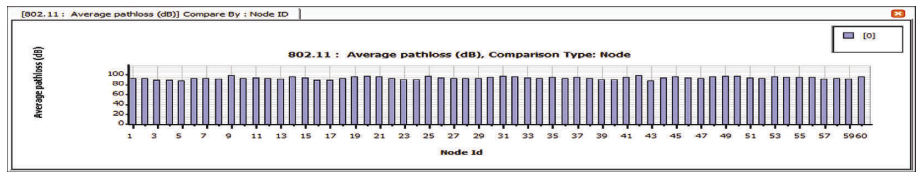


(f)

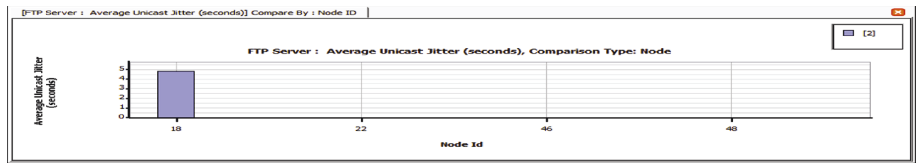


(g)

FIGURE 15: (a) Transmit mode energy consumption of STAR-LORA for FTP deployment. (b) Receive mode energy consumption of STAR-LORA for FTP deployment. (c) Idle mode energy consumption of STAR-LORA for FTP deployment. (d) Average transmission delay of STAR-LORA for FTP deployment. (e) Percentage of utilization of STAR-LORA for FTP deployment. (f) Average pathloss of STAR-LORA for FTP deployment. (g) Average jitter of STAR-LORA for FTP deployment.

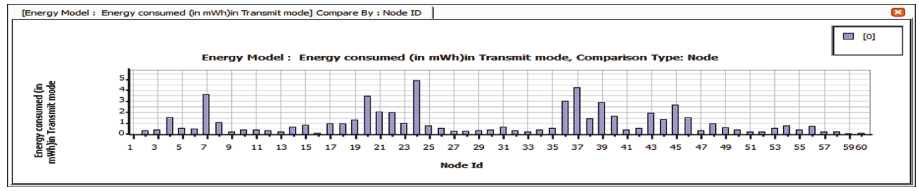


(a)

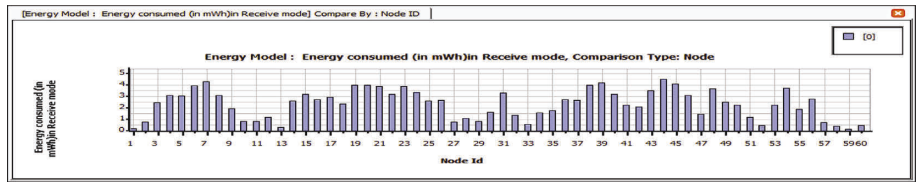


(b)

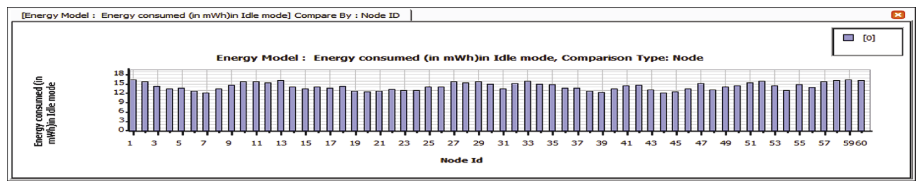


(c)

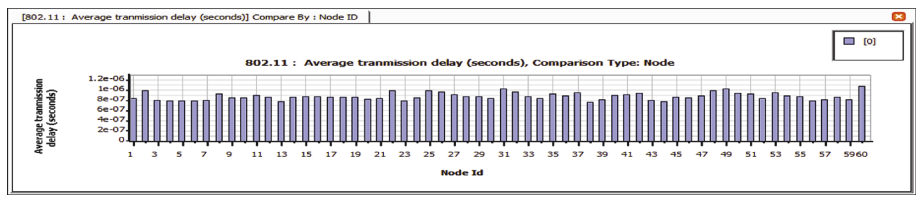


(d)

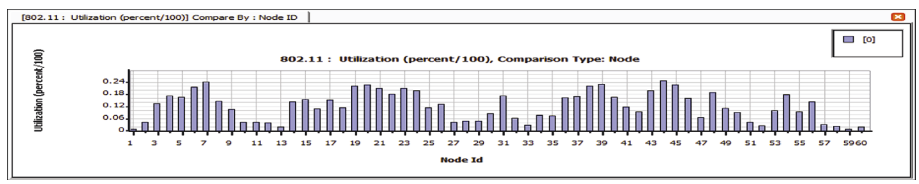


(e)

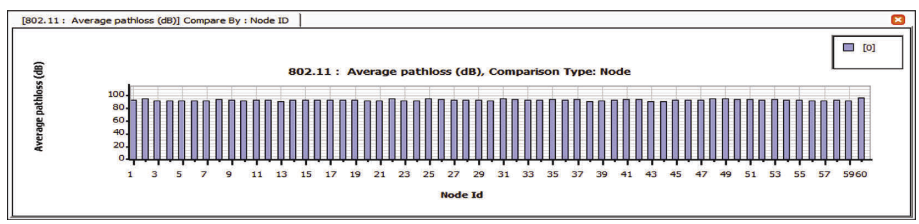


(f)

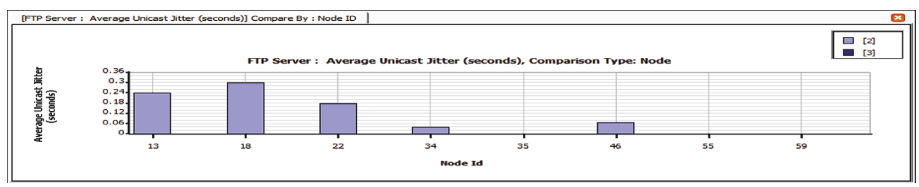


(g)

FIGURE 16: (a) Transmit mode energy consumption of ZRP for FTP deployment. (b) Receive mode energy consumption of ZRP for FTP deployment. (c) Idle mode energy consumption of ZRP for FTP deployment. (d) Average transmission delay of ZRP for FTP deployment. (e) Percentage of utilization of ZRP for FTP deployment. (f) Average pathloss of ZRP for FTP deployment. (g) Average jitter of ZRP for FTP deployment.

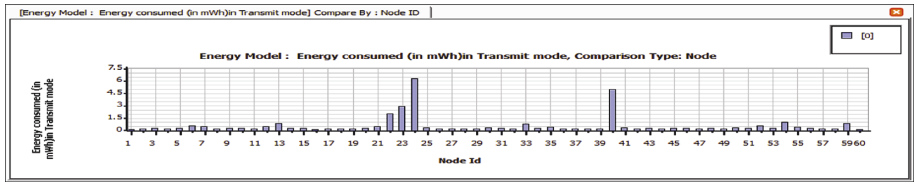


(a)

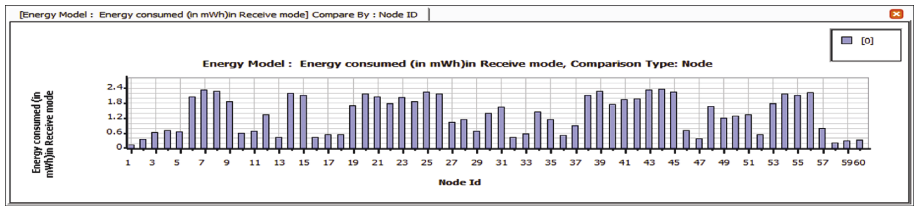


(b)

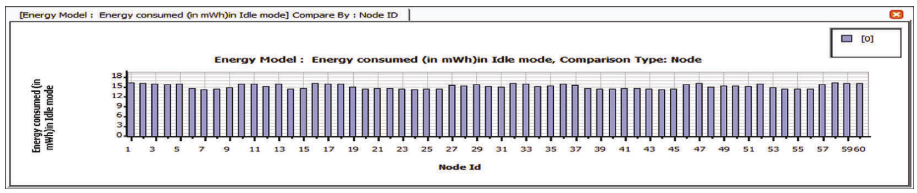


(c)

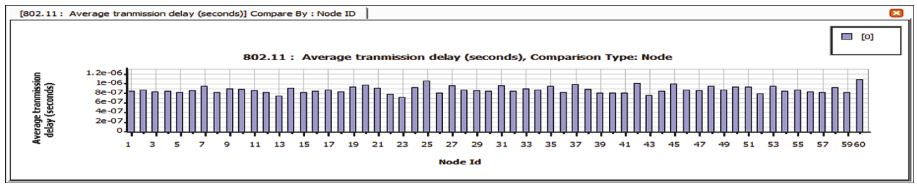


(d)

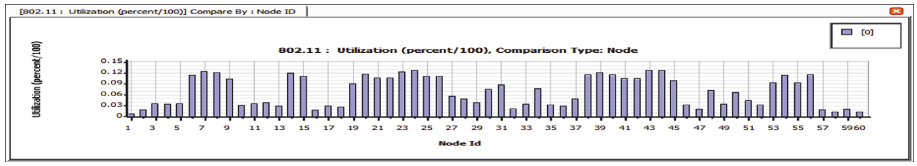


(e)

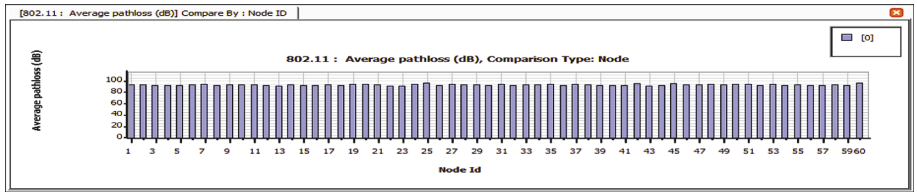


(f)

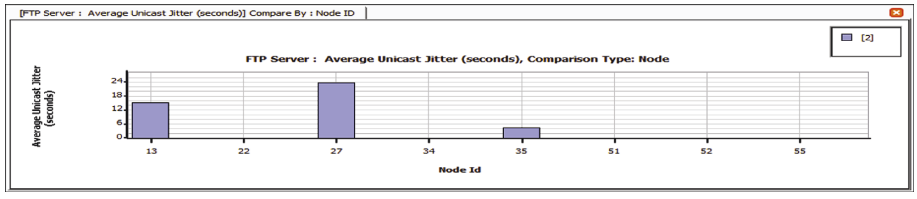


(g)

FIGURE 17: (a) Transmit mode energy consumption of STAR-ORA for FTP deployment. (b) Receive mode energy consumption of STAR-ORA for FTP deployment. (c) Idle mode energy consumption of STAR-ORA for FTP deployment. (d) Average transmission delay of STAR-ORA for FTP deployment. (e) Percentage of utilization of STAR-ORA for FTP deployment. (f) Average pathloss of STAR-ORA for FTP deployment. (g) Average jitter of STAR-ORA for FTP deployment.

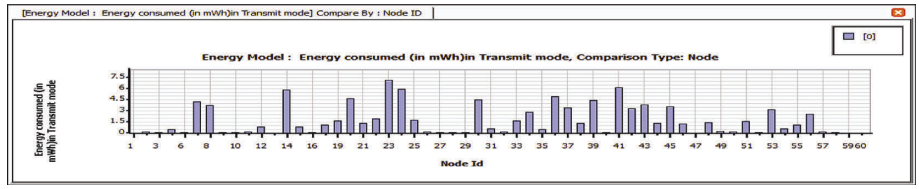


(a)

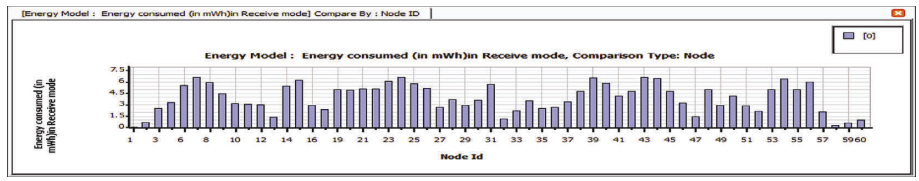


(b)

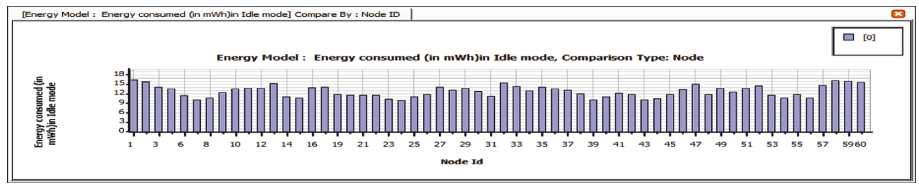


(c)

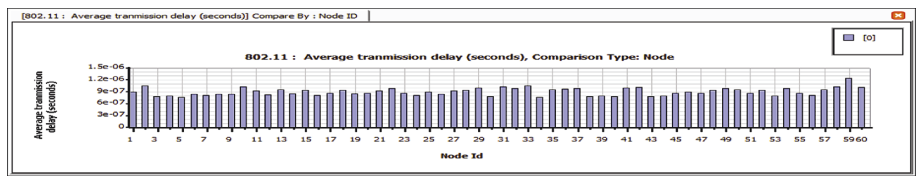


(d)

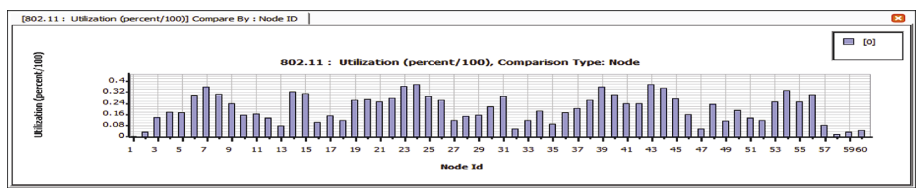


(e)

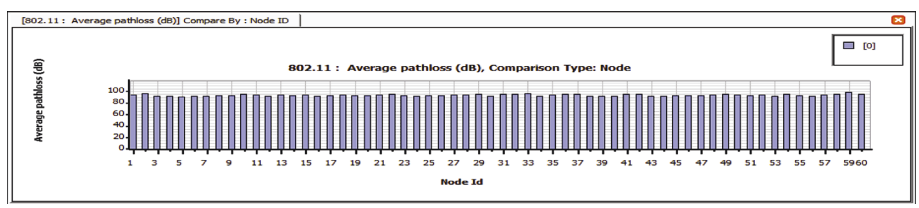


(f)

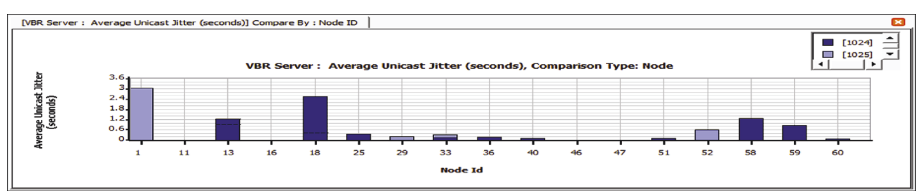


(g)

FIGURE 18: (a) Transmit mode energy consumption of AODV for VBR deployment. (b) Receive mode energy consumption of AODV for VBR deployment. (c) Idle mode energy consumption of AODV for VBR deployment. (d) Average transmission of delay of AODV for VBR deployment. (e) Percentage of utilization of AODV for VBR deployment. (f) Average pathloss of AODV for VBR deployment. (g) Average jitter of AODV for VBR deployment.

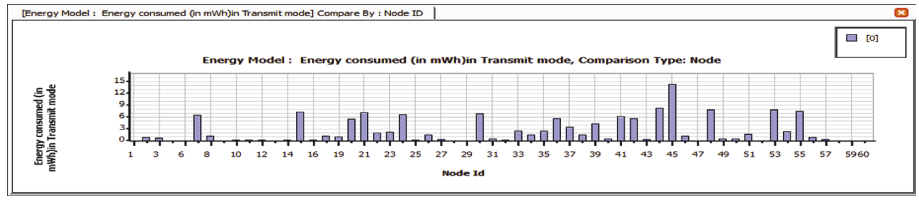


(a)

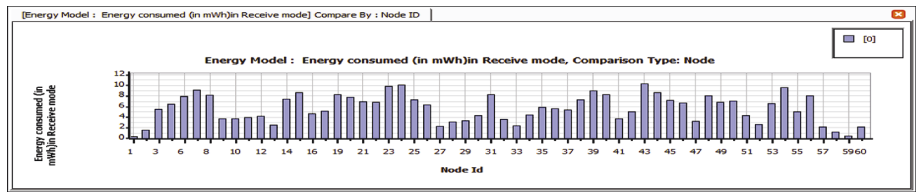


(b)

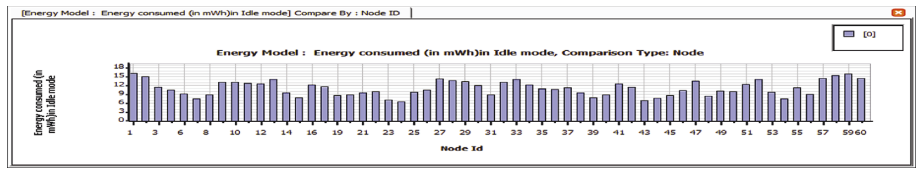


(c)

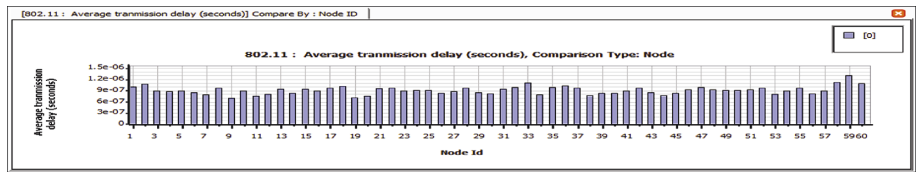


(d)

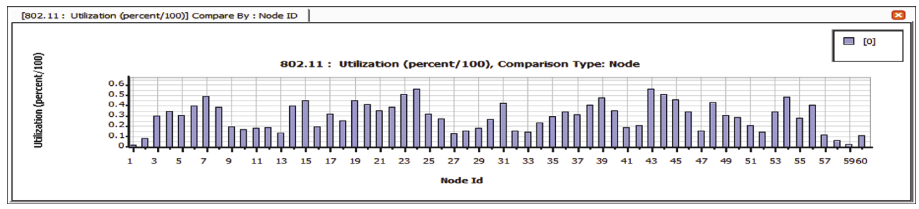


(e)

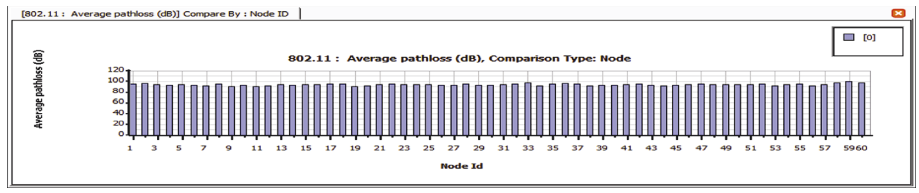


(f)

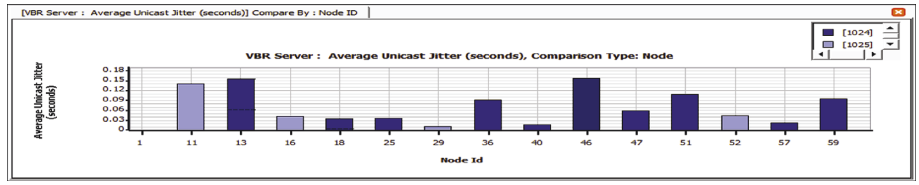


(g)

Figure 19: (a) Transmit mode energy consumption of DSR for VBR deployment. (b) Receive mode energy consumption of DSR for VBR deployment. (c) Idle mode energy cnsumption of DSR for VBR deployment. (d) Average transmission delay of DSR for VBR deployment. (e) Percentage of utilization of DSR for VBR deployment. (f) Average pathloss of DSR for VBR deployment. (g) Average jitter of DSR for VBR deployment.

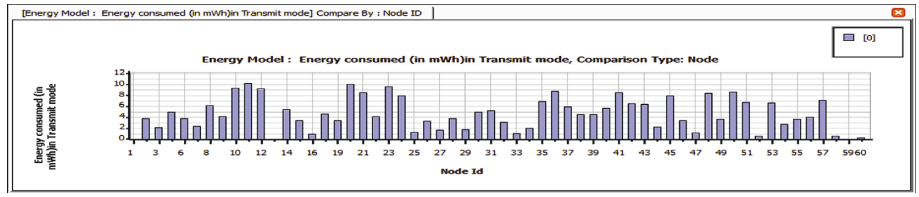


(a)

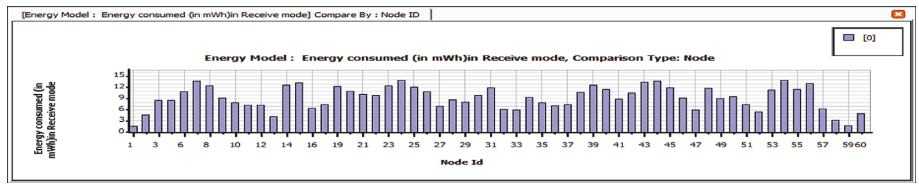


(b)

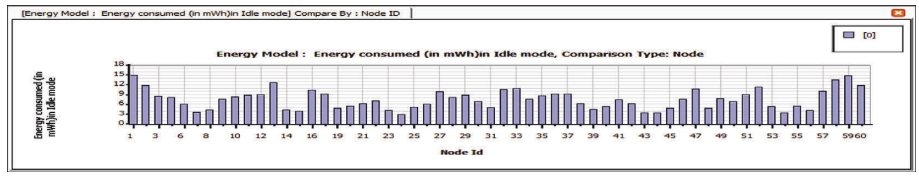


(c)

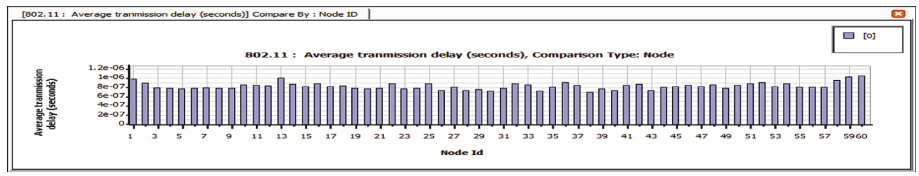


(d)

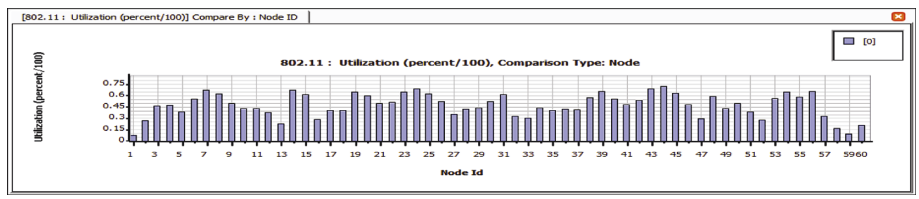


(e)

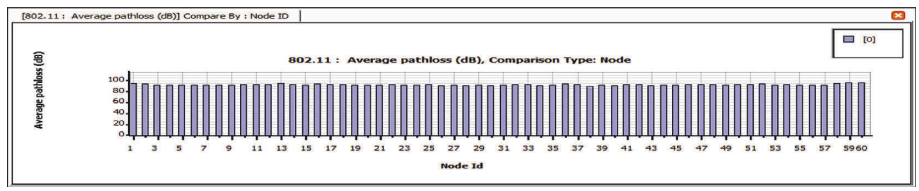


(f)

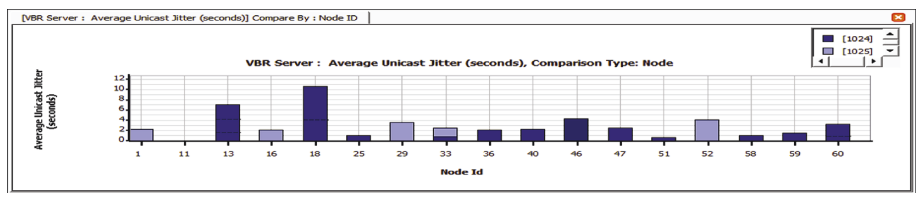


(g)

FIGURE 20: (a) Transmit mode energy consumption of DYMO for VBR deployment. (b) Receive mode energy consumption of DYMO for VBR deployment. (c) Idle mode energy consumption of DYMO for VBR deployment. (d) Average transmission delay of DYMO for VBR deployment. (e) Percentage of utilization of DYMO for VBR deployment. (f) Average pathloss of DYMO for VBR deployment. (g) Average jitter of DYMO for VBR deployment.

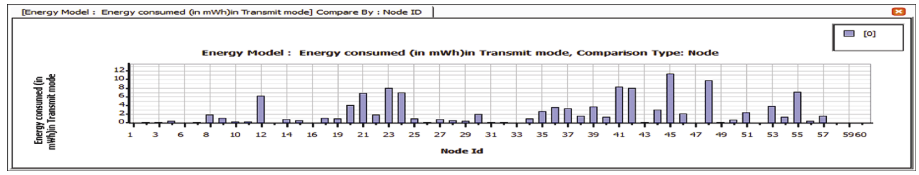


(a)

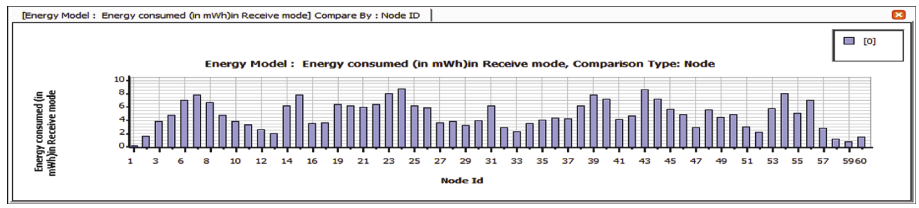


(b)

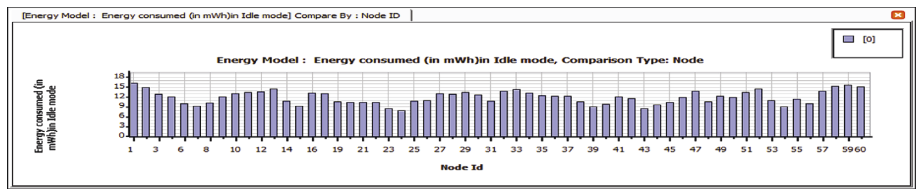


(c)

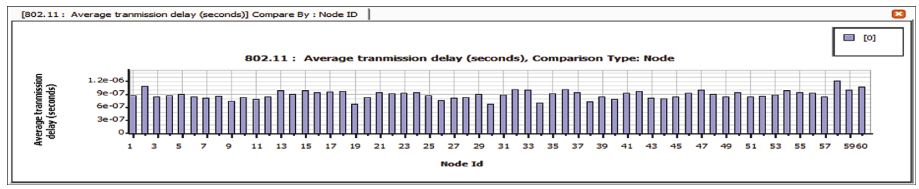


(d)

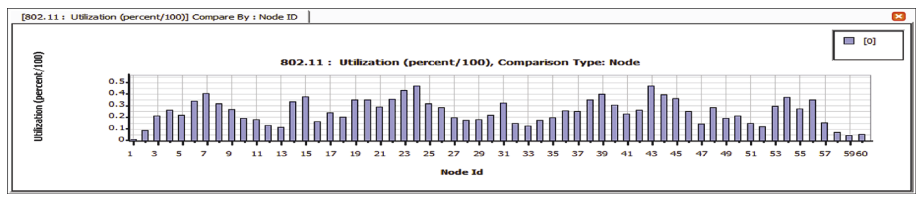


(e)

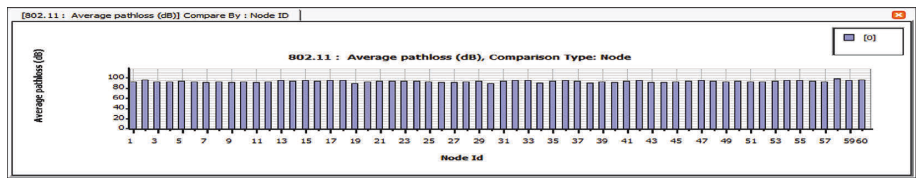


(f)

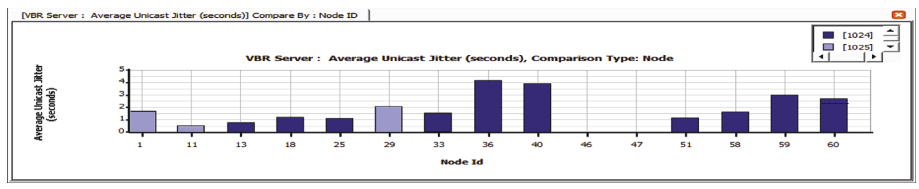


(g)

FIGURE 21: (a) Transmit mode energy consumption of LAR1 for VBR deployment. (b) Receive mode energy consumption of LAR1 for VBR deployment. (c) Idle mode energy consumption of LAR1 for VBR deployment. (d) Average transmission delay of LAR1 for VBR deployment. (e) Percentage of utilization of LAR1 for VBR deployment. (f) Average pathloss of LAR1 for VBR deployment. (g) Average jitter of LAR1 for VBR deployment.

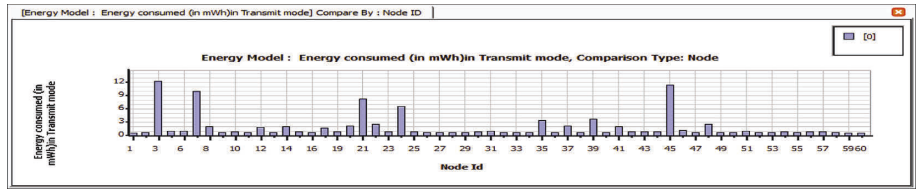


(a)

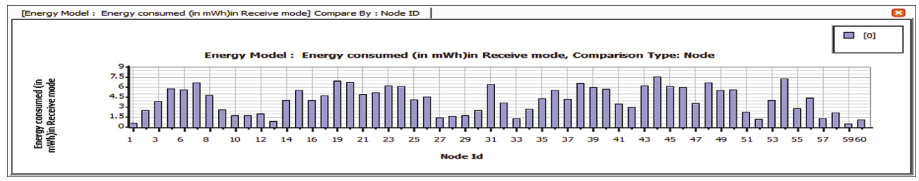


(b)

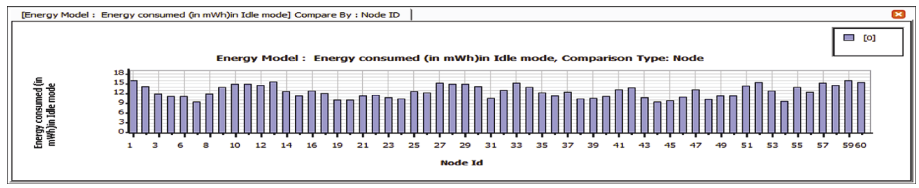


(c)

FIGURE 22: (a) Transmit mode energy consumption of OLSR for VBR deployment. (b) Receive mode energy consumption of OLSR for VBR deployment. (c) Idle mode energy consumption of OLSR for VBR deployment.

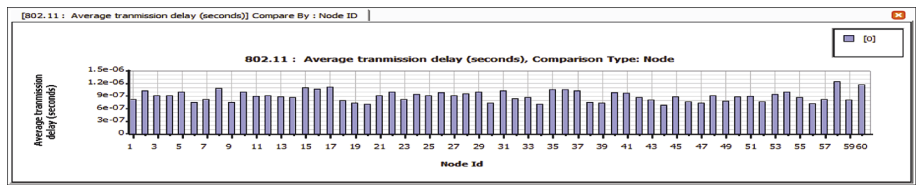


(a)

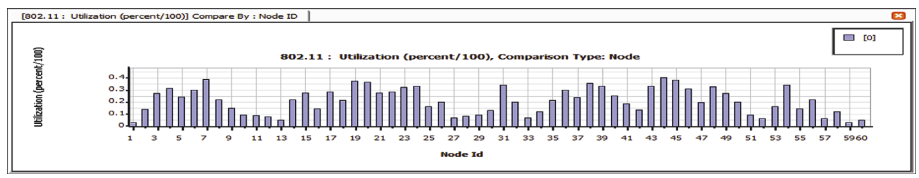


(b)

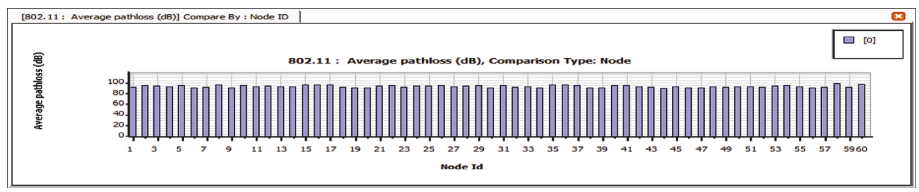


(c)

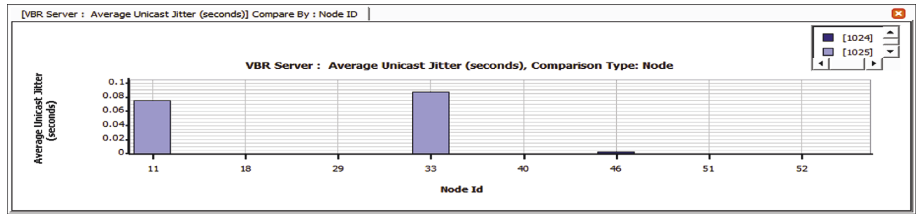


(d)

FIGURE 23: (a) Average transmission delay of OLSR for VBR deployment. (b) Percentage of utilization of OLSR for VBR deployment. (c) Average pathloss of OLSR for VBR deployment. (d) Average jitter of OLSR for VBR deployment.

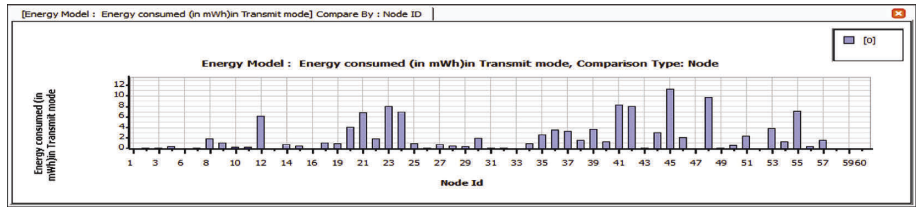


(a)

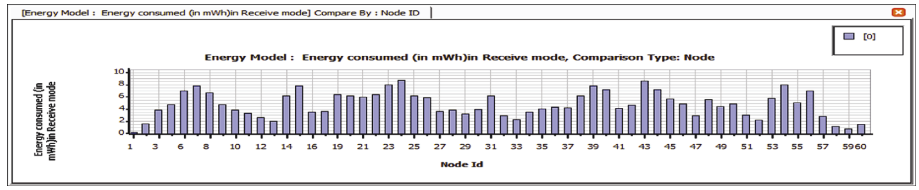


(b)

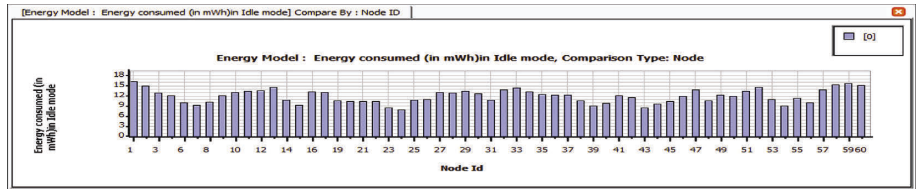


(c)

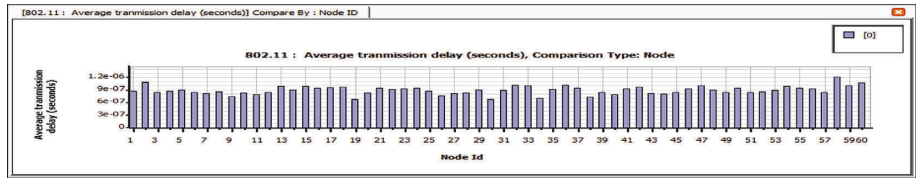


(d)

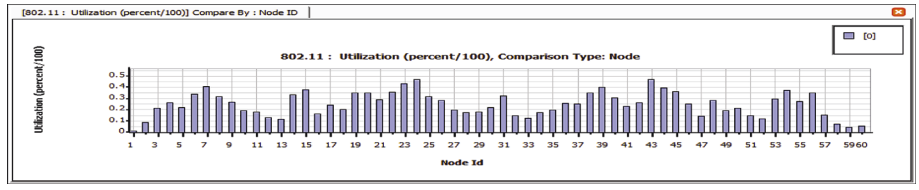


(e)

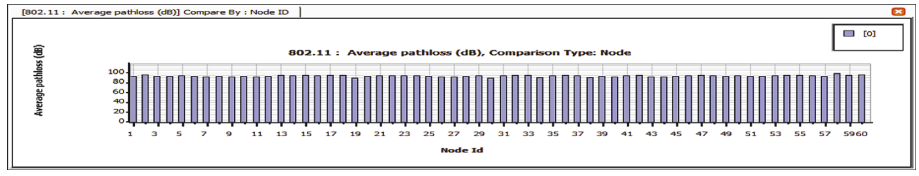


(f)

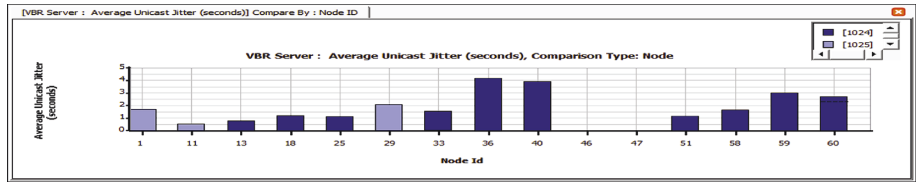


(g)

FIGURE 24: (a) Transmit mode energy consumption of BELLMAN FORD for VBR deployment. (b) Receive mode energy consumption of BELLMAN FORD for VBR deployment. (c) Idle mode energy consumption of BELLMAN FORD for VBR deployment. (d) Average transmission delay of BELLMAN FORD for VBR deployment. (e) Percentage of utilization of BELLMAN FORD for VBR deployment. (f) Average pathloss of BELLMAN FORD for VBR deployment. (g) Average jitter of BELLMAN FORD for VBR deployment.

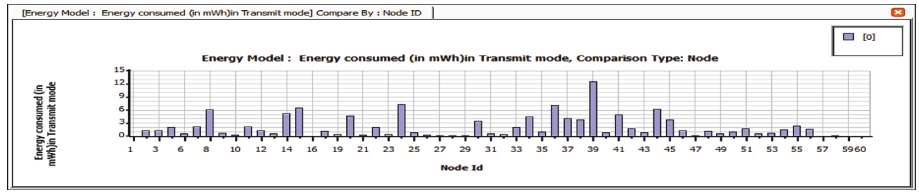


(a)

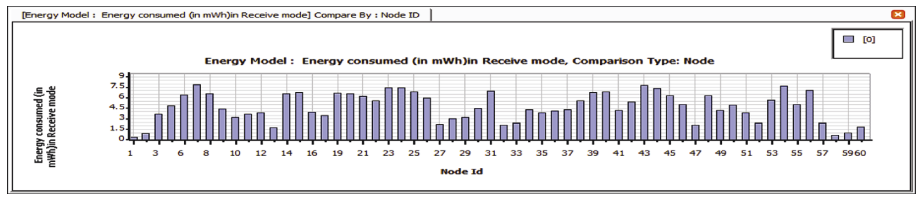


(b)

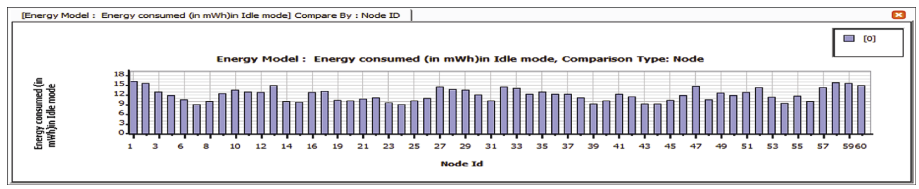


(c)

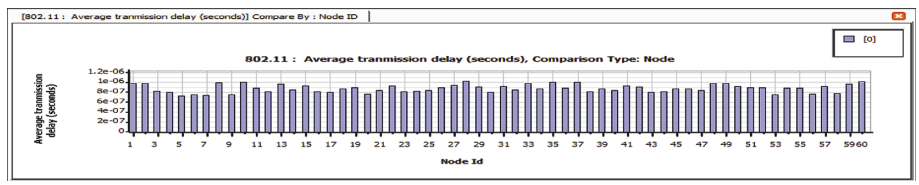


(d)

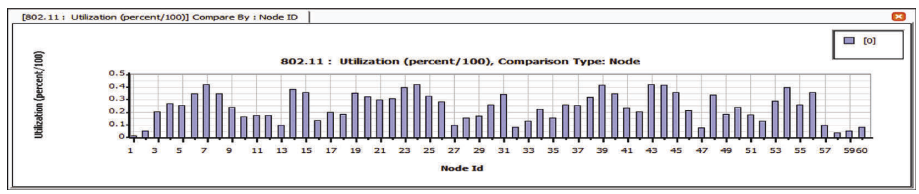


(e)

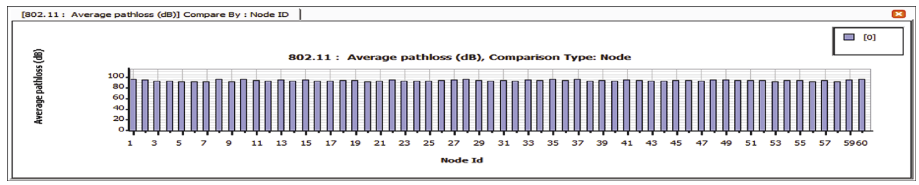


(f)

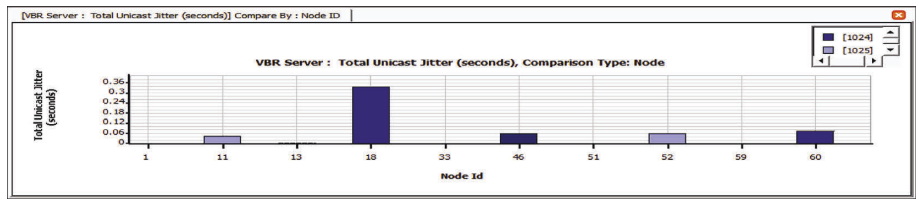


(g)

FIGURE 25: (a)Transmit mode energy consumption of Fisheye for VBR deployment. (b) Receive mode energy consumption of Fisheye for VBR deployment. (c) Idle mode energy consumption of Fisheye for VBR deployment. (d) Average transmission delay of Fisheye for VBR deployment. (e) Percentage of utilization of Fisheye for VBR deployment. (f) Average pathloss of Fisheye for VBR deployment. (g) Average jitter of Fisheye for VBR deployment.

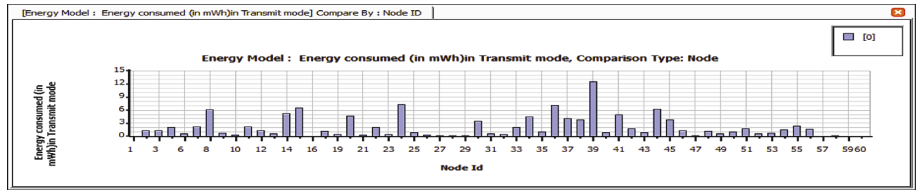


(a)

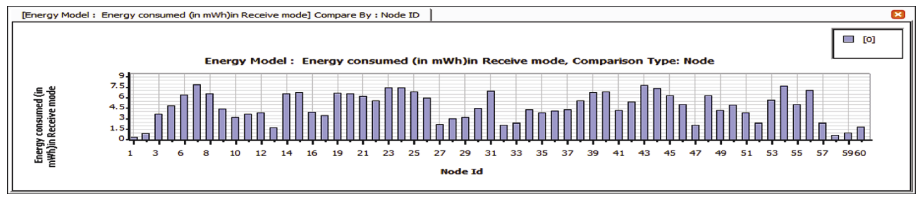


(b)

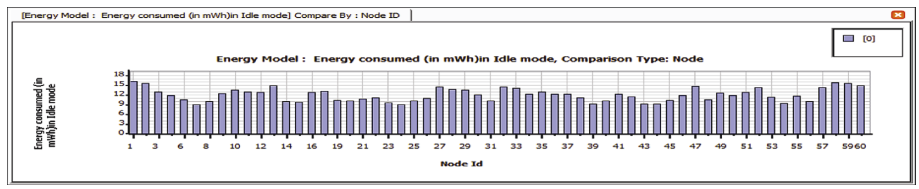


(c)

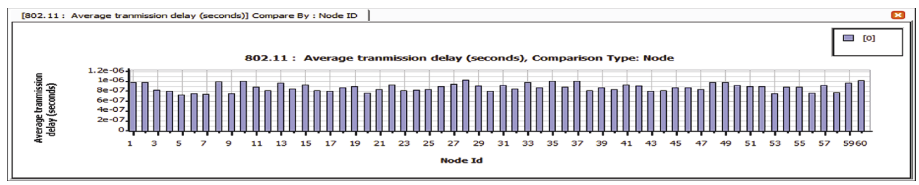


(d)

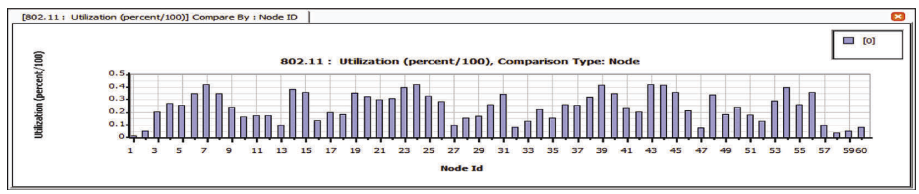


(e)

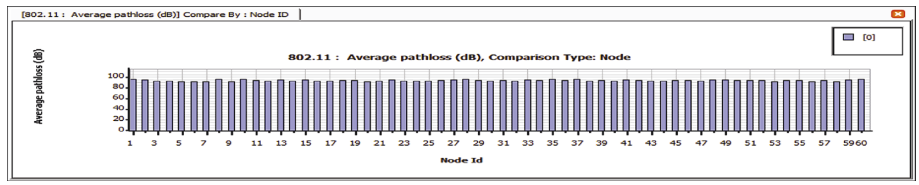


(f)

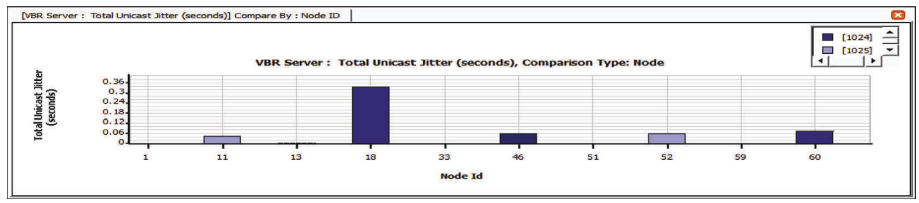


(g)

FIGURE 26: (a) Transmit mode energy consumption of STAR-ORA for VBR deployment. (b) Receive mode energy consumption of STAR-ORA for VBR deployment. (c) Idle mode energy consumption of STAR-ORA for VBR deployment. (d) Average transmission delay of STAR-ORA for VBR deployment. (e) Percentage of utilization of STAR-ORA for VBR deployment. (f) Average pathloss of STAR-ORA for VBR deployment. (g) Average jitter of STAR-ORA for VBR deployment.

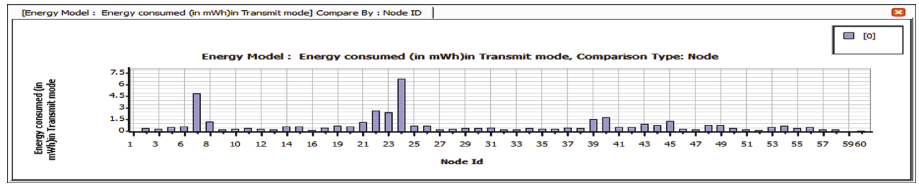


(a)

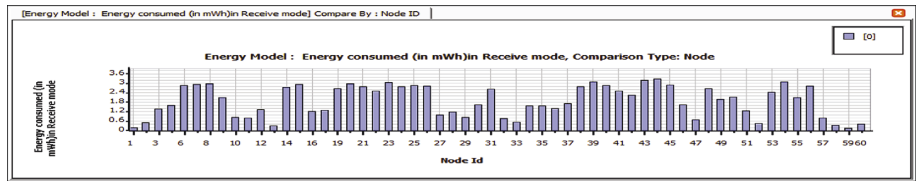


(b)

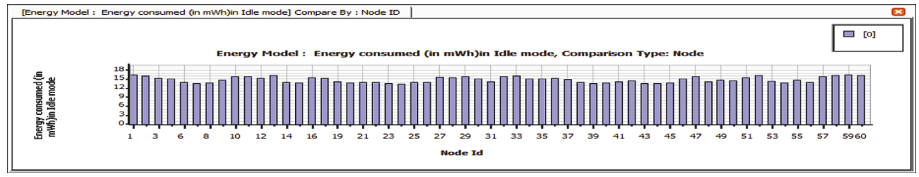


(c)

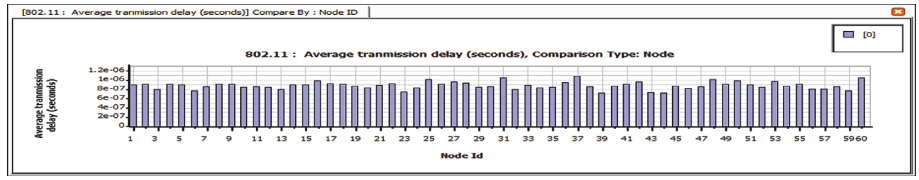


(d)

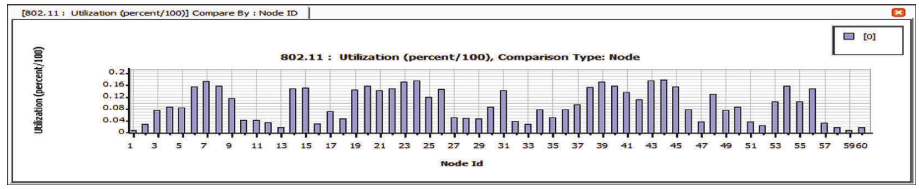


(e)

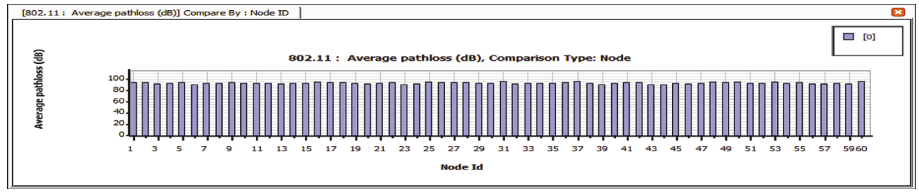


(f)

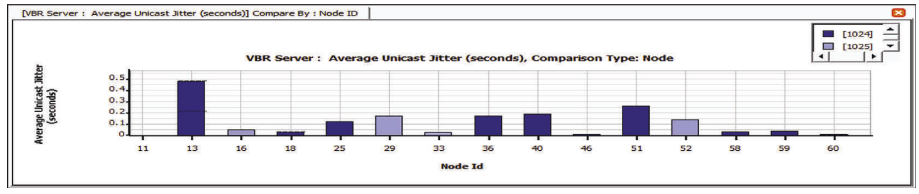


(g)

Figure 27: (a) Transmit mode energy consumption of ZRP for VBR deployment. (b) Receive mode energy consumption of ZRP for VBR deployment. (c) Idle mode energy consumption of ZRP for VBR deployment. (d) Average transmission delay of ZRP for VBR deployment. (e) Percentage utilization of ZRP for VBR deployment. (f) Average pathloss of ZRP for VBR deployment. (g) Average jitter of ZRP for VBR deployment.

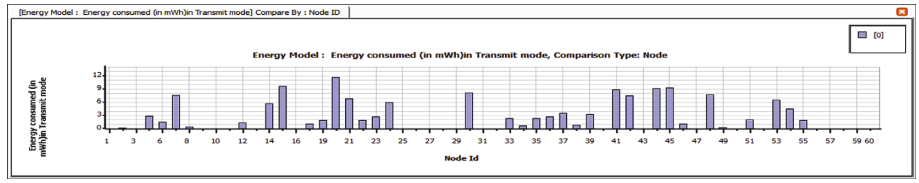


(a)

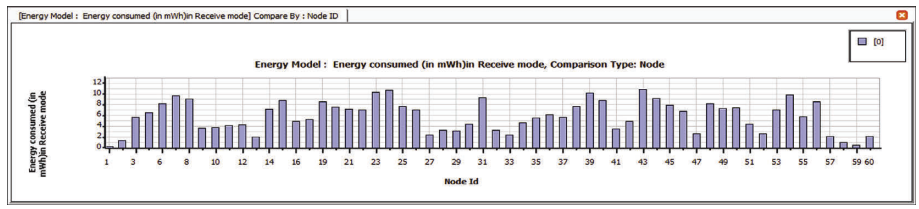


(b)

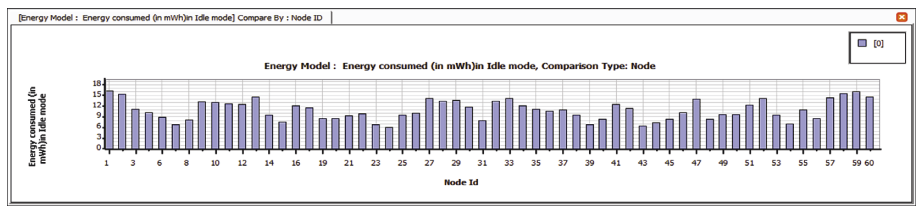


(c)

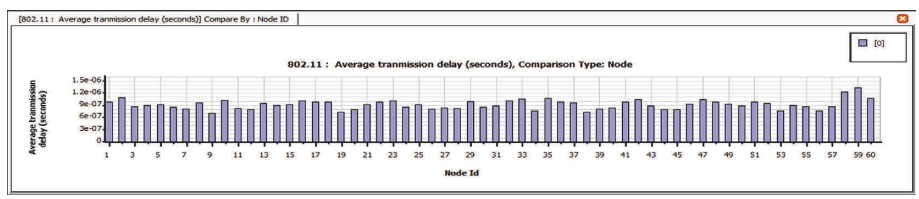


(d)

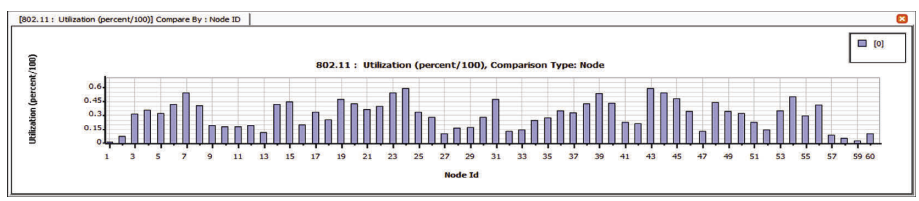


(e)

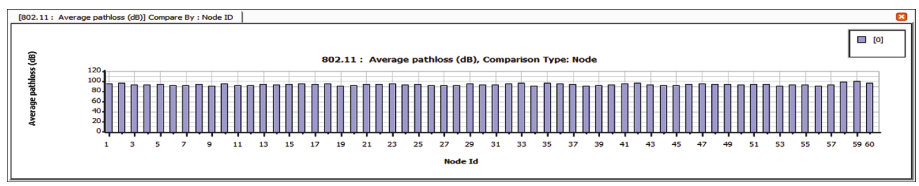


(f)

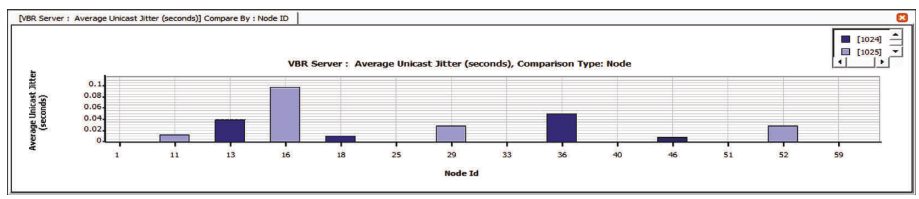


(g)

FIGURE 28: (a) Transmit mode energy consumption of STAR-LORA for VBR deployment. (b) Receive mode energy consumption of STAR-LORA for VBR deployment. (c) Idle mode energy consumption of STAR-LORA for VBR deployment. (d) Average transmission delay of STAR-LORA for VBR deployment. (e) Percentage of utilization of STAR-LORA for VBR deployment. (f) Average pathloss of STAR-LORA for VBR deployment. (g) Average jitter of STAR-LORA for VBR deployment.

LORA routing protocols in transmit mode with FTP, CBR and VBR applications is as shown in Figure 29. In proposed UWSN, minimum transmits energy is consumed on the maximum data size of AODV routing protocol in CBR application by 84.6% of DSR, DYMO, LAR1, Bellman Ford, OLSR, Fisheye, STAR-ORA, ZRP, and STAR-LORA routing protocol, respectively, as illustrated in Table 1. For UWSN, the goal is to use as little transmit energy as possible. Other routing protocols cannot compete against AODV's speed and reliability.

*5.1.2. Energy (Milli Watt Hour-mWh) Consumed in Receive Mode by AODV, DSR, DYMO, LAR1, Bellman Ford, OLSR, Fisheye, STAR-ORA, ZRP, and STAR-LORA Routing Protocols.* Figure 30 presents a comparison of the amount of receive energy consumed by the routing protocols AODV, DSR, DYMO, LAR1, Bellman Ford, OLSR, Fisheye, STAR-ORA, ZRP, and STAR-LORA with FTP, CBR, and VBR applications. When compared to the other routing protocols shown in Table 1, such as DSR, DYMO, LAR1, Bellman Ford, OLSR, Fisheye, STAR-ORA, ZRP, and STAR-LORA, the AODV routing protocol uses 78.5 percent in CBR application and receives less energy than those other protocols. When compared to other routing protocols, the AODV routing protocol consumes significantly and receives less energy than other routing protocols do when dealing with larger packet sizes. UWSN should consume the least amount of energy possible when receiving data. The AODV routing protocol outperforms other routing protocols in terms of performance.z

*5.1.3. Energy (Milli Watt Hour-mWh) Consumed in Idle Mode by AODV, DSR, DYMO, LAR1, Bellman Ford, OLSR, Fisheye, STAR-ORA, ZRP, and STAR-LORA Routing Protocols.* Idle energy consumption by AODV, DSR, DYMO, LAR1, Bellman Ford, OLSR, Fisheye, STAR-ORA, ZRP, and STAR-LORA routing protocols with FTP, CBR, and VBR applications is as shown in Figure 31. Increased packet size reduces the amount of idle energy that must be expended. More energy is saved when using the OLSR routing protocol by 75% instead of the other in CBR application in Table 1, even when sending larger packets. Energy consumption during idle time is undesirable for UWSN. In terms of performance, the OLSR routing protocol is superior to the other protocols in this category.

*5.1.4. Average Transmission Delay (μsec) by AODV, DSR, DYMO, LAR1, Bellman Ford, OLSR, Fisheye, STAR-ORA, ZRP, and STAR-LORA Routing Protocols.* AODV, DSR, DYMO, LAR1, Bellman Ford, OLSR, Fisheye, STAR-ORA, ZRP, and STAR-LORA are compared with one another in terms of their average delay in Figure 32. As can be seen in Table 1, the AODV routing protocol results in an average

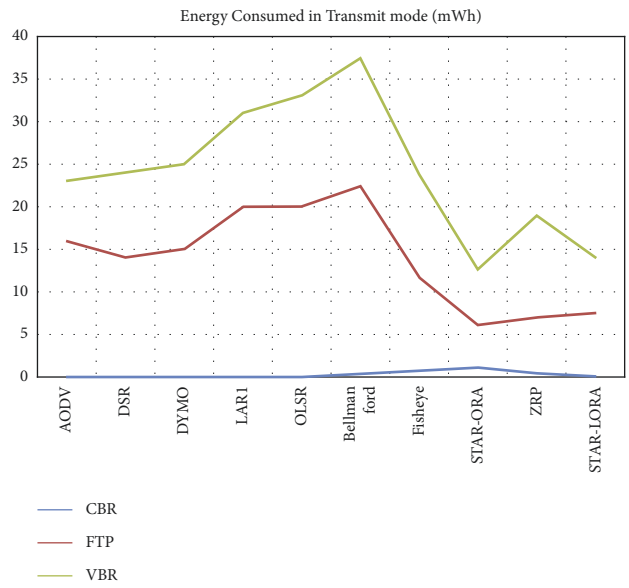


Figure 29: Energy consumed in transmit mode of all routing protocols in CBR, FTP, and VBR applications.

delay that is 89.4 percent shorter than that of other routing protocol in CBR application.

*5.1.5. Percentage of Utilization by AODV, DSR, DYMO, LAR1, Bellman Ford, OLSR, Fisheye, STAR-ORA, ZRP, and STAR-LORA Routing Protocols.* Table 1 shows that the Fisheye routing protocol achieved 92.3 percent higher percentage of utilization in the CBR application than other routing protocols, and Figure 33 shows the percentage of utilization produced by AODV, DSR, DYMO, LAR1, Bellman Ford, OLSR, Fisheye, STAR-ORA, ZRP, and STAR-LORA.

*5.1.6. Average Pathloss (dB) by AODV, DSR, DYMO, LAR1, Bellman Ford, OLSR, Fisheye, STAR-ORA, ZRP, and STAR-LORA Routing Protocols.* The comparison of average Pathloss in current network is shown in Figure 34. DSR achieved 0.3% less average Pathloss in comparison with DSR, DYMO, LAR1, Bellman Ford, OLSR, Fisheye, STAR-ORA, ZRP, and STAR-LORA routing protocols as depicted in Table 1.

*5.1.7. Average Jitter (μsec) by AODV, DSR, DYMO, LAR1, Bellman Ford, OLSR, Fisheye, STAR-ORA, ZRP, and STAR-LORA Routing Protocols.* As shown in Figure 35, each routing protocol has an average latency that is depicted in terms of jitter. When compared to other routing protocols in the proposed network, STAR-LORA produces 86.4 percent less average jitter than the others shown in Table 1.

Table 1 shows the comparison of all routing protocols AODV, DSR, DYMO, LAR1, Bellman Ford, OLSR, Fisheye,

Table 1: Comparison of all routing protocols in CBR, FTP, and VBR applications.

| Parmeter | Protocol | | | | | | | | | | | | | | | | | | | | | | | | | | | | | |
|---|---|---|---|---|---|---|---|---|---|---|---|---|---|---|---|---|---|---|---|---|---|---|---|---|---|---|---|---|---|---|
| | OSLR | | | DSR | | | AODV | | | LAR1 | | | DYMO | | | ZRP | | | STAR-LORA | | | STAR-ORA | | | Fisheye | | | BELLMAN FORD | | |
| | CBR | FTP | VBR | CBR | FTP | VBR | CBR | FTP | VBR | CBR | FTP | VBR | CBR | FTP | VBR | CBR | FTP | VBR | CBR | FTP | VBR | CBR | FTP | VBR | CBR | FTP | VBR | CBR | FTP | VBR |
| Average transmission delay (usec) | 28 | 49 | 39 | 23 | 42 | 36 | 18 | 27 | 35 | 27 | 49 | 42.6 | 31 | 54.8 | 40.5 | 27.9 | 37.5 | 48 | 34.8 | 46 | 53.8 | 30.4 | 38 | 44 | 25 | 45.8 | 48 | 33 | 31 | 43.5 |
| Receive power consumption (mVh) | 0.2 | 14 | 7.5 | 0.2 | 15 | 13 | 0.2 | 8 | 6.5 | 0.1 | 14 | 8.5 | 0.14 | 8 | 8 | 0.65 | 2.5 | 10 | 0.1 | 2 | 3.5 | 0.5 | 4.5 | 1.5 | 1.2 | 9 | 7.5 | 0.3 | 10 | 10 |
| Idle power consumption (mVh) | 0.1 | 15 | 15 | 0.1 | 13 | 15 | 0.1 | 15 | 15 | 0.1 | 15 | 16 | 0.12 | 15 | 17 | 0.16 | 17 | 15 | 0.15 | 15 | 16 | 0.16 | 16 | 17 | 0.15 | 15 | 16 | 0.2 | 15 | 16 |
| Transmit power consumption (mVh) | 0.1 | 20 | 13 | 0.1 | 14 | 10 | 0.1 | 16 | 7 | 0.1 | 20 | 11 | 0.1 | 15 | 10 | 0.55 | 6.5 | 12 | 0.12 | 7.5 | 6.5 | 1.2 | 5 | 6.5 | 0.8 | 11 | 12 | 0.5 | 22 | 15 |
| Percentage of utilization | 0.7 | 0.9 | 0.8 | 0.7 | 0.7 | 0.3 | 0.3 | 0.2 | 0.1 | 0.6 | 0.2 | 0.19 | 0.61 | 0.57 | 0.2 | 0.09 | 0.1 | 0.24 | 0.01 | 0.38 | 0.7 | 0.9 | 0 | 0.2 | 0.09 | 0.17 | 0.2 | 0.1 | 0.2 | 0.25 |
| Average jitter (usec) | 0.4 | 1.1 | 1 | 1.4 | 14 | 26 | 4.9 | 12 | 10 | 5.4 | 17 | 17.9 | 1.08 | 8.4 | 15.6 | 10.1 | 13.5 | 0.27 | 0.11 | 20.8 | 1.85 | 2.35 | 1.1 | 0.1 | 0.43 | 15.6 | 0.7 | 0.6 | 14 | 0.84 |
| Average pathloss (dB) | 27 | 27 | 27 | 26 | 27 | 27 | 26 | 27 | 28 | 26 | 27 | 27.3 | 25.9 | 26.8 | 26.8 | 26.5 | 27.4 | 27.3 | 26.7 | 27.4 | 27.3 | 25.8 | 27 | 27 | 25.8 | 26.8 | 27 | 26 | 27 | 27.1 |

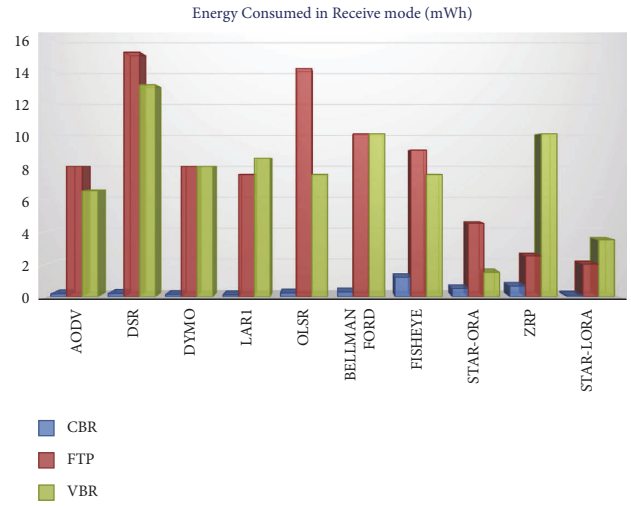


Figure 30: Energy consumed in receive mode of all routing protocols in CBR, FTP, and VBR applications.

STAR-ORA, ZRP, and STAR-LORA when applied to

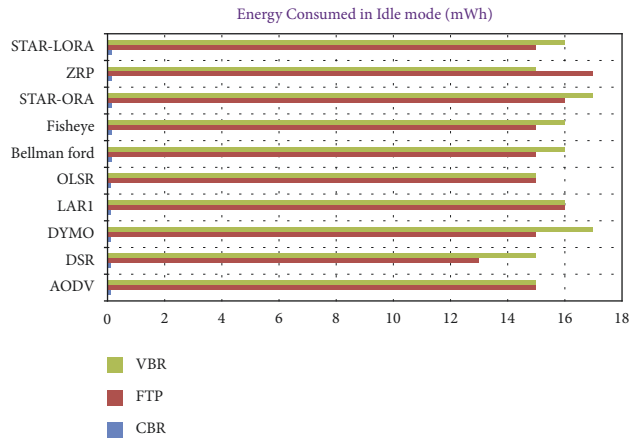


Figure 31: Energy consumed in idle mode of all routing protocols in CBR, FTP, and VBR applications.

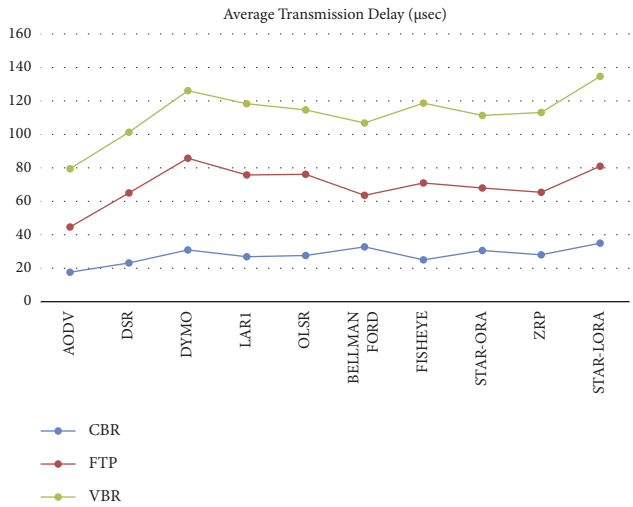


Figure 32: Average transmission delay of all routing protocols in CBR, FTP, and VBR applications.

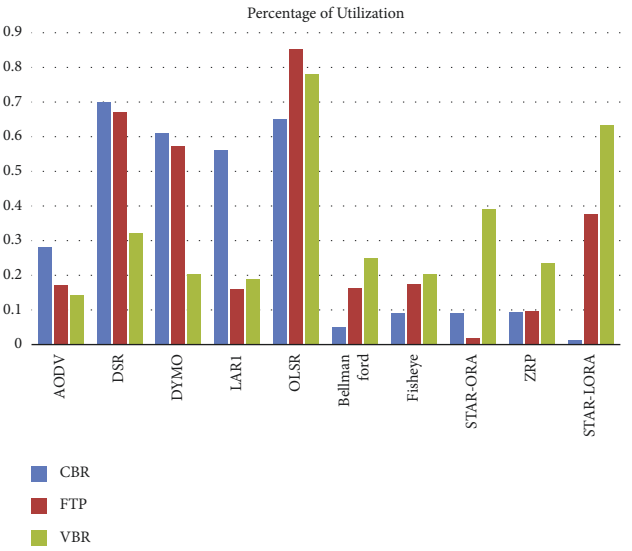


Figure 33: Percentage of utilization of all routing protocols in CBR, FTP, and VBR applications.

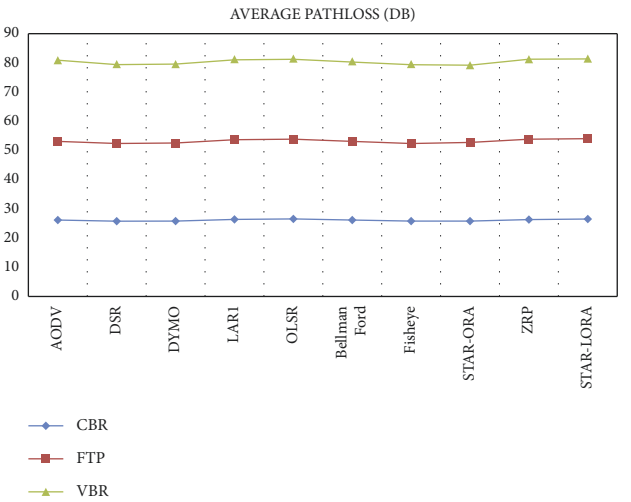


Figure 34: Average pathloss of all routing protocols in CBR, FTP, and VBR applications.

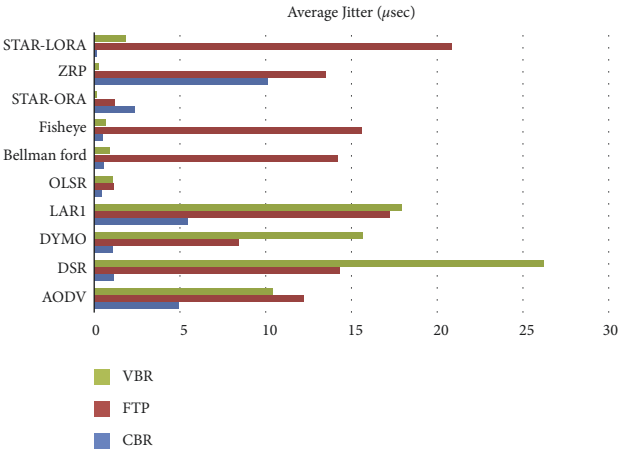


Figure 35: Average jitter of all routing protocols in CBR, FTP, and VBR applications.

UWSN networks with variable deployment applications such as FTP, CBR, and VBR.

## 6. Conclusion

The monitoring of underwater resources, the investigation of parameters, and the planning of military action are all aspects that are developing alongside exploration of an underwater environment. Due to the fact that UWSN is only capable of performing certain tasks, the extent of battery power is the primary focus of the network. Under this paper, we investigate the differences in performance that exist between the routing protocols AODV, DSR, DYMO, LAR1, Bellman Ford, OLSR, Fisheye, STAR-ORA, ZRP, and STAR-LORA when applied to UWSNs with variable deployment applications such as FTP, CBR, and VBR. As performance metrics, we measure things such as the average transmission delay, average jitter, average pathloss, percentage of utilization, and energy consumed in transmit, receive, and idle modes.

According to the findings of our simulations, the AODV routing protocol generates the least amount of total energy when compared to the DSR, DYMO, LAR1, Bellman Ford, OLSR, Fisheye, STAR-ORA, ZRP, and STAR-LORA routing protocols. In addition, the Fisheye routing protocol achieves 92 percent better percentage of utilization than the AODV, DSR, DYMO, LAR1, Bellman Ford, OLSR, Fisheye, STAR-ORA, ZRP, and STAR-LORA routing protocols, and the DSR produces 0.3 percent better average path loss. Finally, STAR-LORA produces 86.4 percent less average jitter than the other routing protocols.

## Abbreviations

| | |
|---|---|
| AODV: | Ad-hoc On-demand Distance Vector |
| ZRP: | Zone Routing Protocol |
| DSR: | Dynamic source routing protocol |
| FSR: | Fisheye State Routing |
| DYMO: | Dynamic MANET on Demand Routing Protocol |
| LAR: | Location Aided Routing |
| OLSR: | Optimized Link State Routing Protocol |
| STAR: | Source Tree Adaptive Routing |
| STAR-ORA: | Source Tree Adaptive Routing Optimum routing approach |
| STAR-LORA: | Source Tree Adaptive Routing Least overhead routing approach. |

## Data Availability

The data used to support the findings of this study are available from the corresponding author upon request (head.sp@bluecrest.edu.lr).

## Conflicts of Interest

The authors declare that they have no conflicts of interest to report regarding the present study.

## Authors' Contributions

K. Sathish conceptualized the study, performed data curation and formal analysis, proposed methodology, provided software, and wrote the original draft. Dr. Asadi Srinivasulu supervised the study, reviewed and edited the manuscript, was responsible for project administration, and visualized the study. Dr. Ravikumar CV visualized the study, investigated the study, performed formal analysis, and provided software. Mr. Anand Kumar Gupta performed data curation, investigated the study, was responsible for resources, provided software, wrote the original draft, and proposed methodology.

## References

[1] S. Fang, "An integrated system for regional environmental monitoring and management based on internet of things," *IEEE Transactions on Industrial Informatics*, vol. 10, no. 2, pp. 1596–1605, 2014.

[2] J. G. Proakis, E. M. Sozer, J. A. Rice, and M. Stojanovic, "Shallow water acoustic networks," *IEEE Communications Magazine*, vol. 39, no. 11, pp. 114–119, 2001.

[3] J. Heidemann, W. Ye, J. Wills, A. Syed, and Y. Li, "Research challenges and applications for underwater sensor networking," *Wireless Communications and Networking Conference*, vol. 1, pp. 228–235, 2006.

[4] S. Rani, S. H. Ahmed, J. Malhotra, and R. Talwar, "Energy efficient chain based routing protocol for underwater wireless sensor networks," *Journal of Network and Computer Applications*, vol. 92, pp. 42–50, 2017.

[5] N. Subramani, P. Mohan, Y. Alotaibi, S. Alghamdi, and O. I. Khalaf, "An efficient metaheuristic-based clustering with routing protocol for underwater wireless sensor networks," *Sensors*, vol. 22, no. 2, p. 415, 2022.

[6] P. Mohan, N. Subramani, Y. Alotaibi, S. Alghamdi, O. I. Khalaf, and S. Ulaganathan, "Improved metaheuristics-based clustering with multihop routing protocol for underwater wireless sensor networks," *Sensors*, vol. 22, no. 4, Article ID 1618, 2022.

[7] M. Ayaz, I. Baig, A. Abdullah, and I. Faye, "A survey on routing techniques in underwater wireless sensor networks," *Journal of Network and Computer Applications*, vol. 34, no. 6, pp. 1908–1927, 2011.

[8] N. Meratnia, "CLAM—collaborative embedded networks for submarine surveillance: an overview," in *Proceedings of the OCEANS, 2011 IEEE-Spain*, pp. 1–4, IEEE, Santander, Spain, June 2011.

[9] E. M. Sozer, M. Stojanovic, and J. G. Proakis, "Underwater acoustic networks," *IEEE Journal of Oceanic Engineering*, vol. 25, no. 1, pp. 72–83, 2000.

[10] J. H. Cui, J. Kong, M. Gerla, and S. Zhou, "The challenges of building mobile underwater wireless networks for aquatic applications," *IEEE Network*, vol. 20, no. 3, pp. 12–18, 2006.

[11] K. Wang, H. Gao, X. Xu, J. Jiang, and D. Yue, "An energy-efficient reliable data transmission scheme for complex environmental monitoring in underwater acoustic sensor networks," *IEEE Sensors Journal*, vol. 16, no. 11, pp. 4051–4062, 2016.

[12] G. Han, J. Jiang, L. Shu, and M. Guizani, "An attack-resistant trust model based on multidimensional trust metrics in underwater acoustic sensor network," *IEEE Transactions on Mobile Computing*, vol. 14, no. 12, pp. 2447–2459, 2015.

[13] R. Agarwal, S. Kumar, and R. M. Hegde, "Algorithms for crowd surveillance using passive acoustic sensors over a multimodal sensor network," *IEEE Sensors Journal*, vol. 15, no. 3, pp. 1920–1930, 2015.

[14] G. Han, J. Jiang, L. Shu, Y. Xu, and F. Wang, "Localization algorithms of underwater wireless sensor networks: a survey," *Sensors*, vol. 12, no. 2, pp. 2026–2061, 2012.

[15] S. Lee and D. Kim, "Underwater hybrid routing protocol for UWSNs," in *Proceedings of the Fifth International Conference on Ubiquitous and Future Networks (ICUFN)*, IEEE, Da Nang, Vietnam, 2013.

[16] F. Yuan, Y. Zhan, and Y. Wang, "Data density correlation degree clustering method for data aggregation in WSN," *IEEE Sensors Journal*, vol. 14, no. 4, pp. 1089–1098, 2014.

[17] C. V. Ravikumar, "Design of MC-CDMA receiver using RBF network to mitigate MAI and non linear distortion," *Neural Computing & Applications*, vol. 31, no. 2, 2019.

[18] S. Rani, R. Talwar, J. Malhotra, S. H. Ahmed, M. Sarkar, and H. Song, "A novel scheme for an energy efficient Internet of Things based on wireless sensor networks," *Sensors*, vol. 15, no. 11, pp. 28603–28626, 2015.

[19] C. Perkins, E. Belding-Royer, and S. Das, *Ad hoc on-Demand Distance Vector (AODV) Routing*, https://en.wikipedia.org/wiki/Ad_hoc_On-Demand_Distance_Vector_Routing, 2003.

[20] S. H. Manjula, C. N. Abhilash, K. Shaila, K. R. Venugopal, and L. M. Patnaik, "Performance of AODV routing protocol using group and entity mobility models in wireless sensor networks," *International Multi Conference of Engineers and Computer Scientist*, vol. 2, pp. 1212–1217, 2008.

[21] G. S. Teja and P. Samundiswary, "Performance analysis of DYMO protocol for IEEE 802.15. 4 based WSNs with mobile nodes," in *Proceedings of the Computer Communication and Informatics (ICCCI)*, IEEE, Coimbatore, India, 2014.

[22] M. K. Park and V. Rodoplu, "UWAN-MAC: an energy-efficient MAC protocol for underwater acoustic wireless sensor networks," *IEEE Journal of Oceanic Engineering*, vol. 32, no. 3, pp. 710–720, 2007.

[23] M. C. Domingo and R. Prior, "Energy analysis of routing protocols for underwater wireless sensor networks," *Computer Communications*, vol. 31, no. 6, pp. 1227–1238, 2008.

[24] C. V. Ravikumar, "MC-CDMA receiver design using recurrent neural network for eliminating MAI and non linear distortion," *International Journal of Communication Systems*, vol. 10, no. 16, 2017.

[25] Z. Alkindi, N. Alzeidi, and B. A. A. Touzene, "Performance evolution of grid based routing protocol for underwater wireless sensor networks under different mobile models," *International Journal of Wireless & Mobile Networks*, vol. 10, no. 1, pp. 13–25, 2018.

[26] M. S. A. Patil and M. P. Mishra, "Improved mobicast routing protocol to minimize energy consumption for underwater wireless sensor networks," *International Journal of Research Science. Engineering.*vol. 3, no. 2, pp. 197–204, 2017.

[27] A. Khan, I. Ahmedy, M. Anisi et al., "A localization-free interference and energy holes minimization routing for underwater wireless sensor networks," *Sensors*, vol. 18, no. 2, p. 165, 2018.

[28] L. E. Emokpae, S. DiBenedetto, B. Potteiger, and M. Younis, "UREAL: underwater reflection enabled acoustic-based localization," *IEEE Sensors Journal*, vol. 14, no. 11, pp. 3915–3925, 2014.

[29] Q. Liang, B. Zhang, C. Zhao, and Y. Pi, "TDoA for passive localization: underwater versus terrestrial environment," *IEEE Transactions on Parallel and Distributed Systems*, vol. 24, no. 10, pp. 2100–2108, 2013.

[30] Z. Yu, C. Xiao, and G. Zhou, "Multi-objectivization-based localization of underwater sensors using magnetometers," *IEEE Sensors Journal*, vol. 14, no. 4, pp. 1099–1106, 2014.

[31] R. Diamant and L. Lampe, "Underwater localization with time-synchronization and propagation speed uncertainties," *IEEE Transactions on Mobile Computing*, vol. 12, no. 7, pp. 1257–1269, 2013.

[32] P. V. Rajaram and M. Prakash, "Intelligent deep learning based bidirectional long short term memory model for automated reply of e-mail client prototype," *Pattern Recognition Letters*, vol. 152, pp. 340–347, 2021.

[33] S. Mishra and M. Prakash, "Digital mammogram inferencing system using intuitionistic fuzzy theory," *Computer Systems Science and Engineering*, vol. 41, no. 3, pp. 1099–1115, 2022.

[34] X. Ba, L. Jin, Z. Li, J. Du, and S. Li, "Multiservice-based traffic scheduling for 5G access traffic steering, switching and splitting," *Sensors*, vol. 22, no. 9, Article ID 3285, 2022.

[35] M. Alsulami, R. Elfouly, and R. Ammar, "A re- liable underwater computing system," in *Proceedings of the 2021 4th IEEE International Conference on Industrial Cyber- Physical Systems (ICPS)*, IEEE, Victoria, BC, Canada, 2021.

[36] K. Bhattacharjya, S. Alam, and D. De, "Performance analysis of DYMO, ZRP and AODV routing protocols in a multi hop grid based underwater wireless sensor network," in *Proceedings of the 2nd International Conference on Computational Intelligence, Communications and Business Analytics (CICBA)*, Springer Nature, Singapore, (2018a).

[37] K. Bhattacharjya, S. Alam, and D. De, "TTCBT: two tier complete binary tree based wireless sensor network for FSR and LANMAR routing protocols," *Microsystem Technologies*, vol. 27, no. 2, pp. 443–453, 2018b.

[38] P. K. Varshney, G. S. Agrawal, and S. K. Sharma, "Relative performance analysis of proactive routing protocols in wireless ad hoc networks using varying node density," *Invertis Journal of Science & Technology*, vol. 9, no. 3, pp. 161–169, 2016.

[39] K. Bhattacharjya, S. Alam, and D. De, "CUWSN: energy efficient routing protocol selection for cluster based underwater wireless sensor network," *Microsystem Technologies*, vol. 28, 2019.

[40] S. Alam and D. De, "Cloud smoke sensing model for AODV, RIP and STAR routing protocols using wireless sensor network in industrial township area," in *Proceedings of the Second International Conference on Research in Computational Intelligence and Communication Networks (ICRCICN)*, IEEE, Kolkata, India, 2016.